© 2019. Published by The Company of Biologists Ltd | Development (2019) 146, dev173377. doi:10.1242/dev.173377

STEM CELLS AND REGENERATION

RESEARCH ARTICLE

Paf1c defects challenge the robustness of flower meristem termination in *Arabidopsis thaliana*

Kateryna Fal*, Matthieu Cortes*, Mengying Liu, Sam Collaudin, Pradeep Das, Olivier Hamant‡ and Christophe Trehin‡

ABSTRACT

Although accumulating evidence suggests that gene regulation is highly stochastic, genetic screens have successfully uncovered master developmental regulators, questioning the relationship between transcriptional noise and intrinsic robustness of development. To identify developmental modules that are more or less resilient to large-scale genetic perturbations, we used the *Arabidopsis* polymerase II-associated factor 1 complex (Paf1c) mutant *vip3*, which is impaired in several RNA polymerase II-dependent transcriptional processes. We found that the control of flower termination was not as robust as classically pictured. In angiosperms, the floral female organs, called carpels, display determinate growth: their development requires the arrest of stem cell maintenance. In *vip3* mutant flowers, carpels displayed a highly variable morphology, with different degrees of indeterminacy defects up to wild-type size inflorescence emerging from carpels. This phenotype was associated with variable expression of two key regulators of flower termination and stem cell maintenance in flowers, *WUSCHEL* and *AGAMOUS*. The phenotype was also dependent on growth conditions. Together, these results highlight the surprisingly plastic nature of stem cell maintenance in plants and its dependence on Paf1c.

KEY WORDS: Floral determinacy, Transcriptional noise, Paf1 complex, *WUSCHEL*, *AGAMOUS*, Carpel, Stem cell, Variability, Developmental robustness

INTRODUCTION

Developmental robustness is ambivalent: patterns of growth must be reproducible, as body plans are usually comparable within individuals of given species; they must also be plastic to enable adaption to external and internal changes and fluctuations. In other words, developmental robustness entails a balance between homeostatic mechanisms that ensure that many phenotypes are robust to genetic and environmental variations and promotion of variability to trigger alternative developmental pathways to face genetic and environmental variations. This balance is also a variable, as the ratio between reproducibility and variability promotion can shift as development progresses (see, for example, Tsugawa et al., 2017).

Among the factors behind developmental robustness, transcriptional noise can contribute to specific differentiation pathways in various tissues (Mason et al., 2014; Mantsoki et al., 2016; Alemu et al., 2014; Padovan-Merhar and Raj, 2013; Sprinzak et al., 2010). In addition, the maintenance of stem cells might rely on the relative inefficiency of the transcriptional and translational machinery that maintains the stem cells in an indeterminate state (Momiji and Monk, 2009). Interestingly, variability of gene expression can account for reduced penetrance (Raj et al., 2010). In plants, the contribution of gene expression variability to plant developmental robustness and plasticity remains poorly documented. Gene expression variability has mainly been assessed during responses to external or internal stimuli (Waters et al., 2017; Xu et al., 2016; Wang et al., 2011) and only more recently as an internal input to support developmental plasticity at the tissue level (Meyer et al., 2017).

Although the exact mechanisms behind transcriptional noise remain to be uncovered, relevant molecular factors are starting to be identified. For instance, the variability of gene expression in mammals relies on several features of the gene itself, spanning from its genomic structure and regulation to its interacting network (Alemu et al., 2014). Interestingly, the RNA polymerase II-associated factor 1 complex (Paf1c) seems to play a key role in this process. Mutations in Paf1c subunits increase gene expression noise in yeast (Ansel et al., 2008; Richard and Yvert, 2014). This effect not only relies on the functional interaction with RNA polymerase II, but also on a larger spectrum of activities. In plants, Paf1c has been shown to influence gene expression through regulation of transcription (Oh et al., 2004; Antosz et al., 2017) and modification of chromatin (He et al., 2004; Oh et al., 2008). In mammals, Paf1c also restrains the activation of enhancers and thus hinders the release of paused RNA polymerase II, adding another layer of control of gene expression variability (Chen et al., 2017). In principle, mutations in Paf1c subunits offer the ideal context for analyzing the role of transcriptional noise in development.

One of the Paf1c components, VERNALIZATION INDEPENDENCE 3 (VIP3), was initially shown to control flowering time (Zhang et al., 2003). Recently, *vip3* mutants were found to exhibit variable phyllotactic patterns: *vip3* mutants exhibit an average divergence angle of 137° between each organ initiation at the shoot apex, as in the wild type, but the standard deviation of that angle is increased in the mutant (Fal et al., 2017). Because no other mutant exhibits such a phenotype, this finding suggests that Paf1c-dependent transcriptional control is important for developmental robustness as a whole. Here, we investigate whether flower termination, a developmental process that is both central to plant reproduction and very reproducible, also depends on Paf1c.

Laboratoire de Reproduction et Développement des Plantes, Université de Lyon, UCB Lyon 1, ENS de Lyon, INRA, CNRS, 46 Allée d'Italie, 69364 Lyon Cedex 07, France.
*These authors contributed equally to this work

‡Authors for correspondence (christophe.trehin@ens-lyon.fr; olivier.hamant@ens-lyon.fr)

O.H., 0000-0001-6906-6620; C.T., 0000-0003-4045-6160

Received 1 November 2018; Accepted 11 September 2019

Development (2019) 146, dev173377. doi:10.1242/dev.173377

Flowers are produced by the shoot apical meristem (SAM), which hosts a pool of pluripotent stem cells. This explains why the SAM at the tip of an inflorescence stem produces an indeterminate number of flowers (Besnard et al., 2011). Young flowers also exhibit early meristematic activity but, in contrast to the SAM, they produce a determinate number of organs (four sepals, four petals, six stamens and two carpels in *Arabidopsis thaliana*). This implies that maintenance of the stem cell pool stops as the flower matures. Two decades of molecular genetics have demonstrated that stem cell homeostasis relies on a negative feedback loop involving the WUSCHEL (WUS) and CLAVATA (CLV) factors (Somssich et al., 2016). *WUS* encodes a homeodomain transcription factor and is expressed deep inside the SAM, in the organizing center (Mayer et al., 1998). The WUS protein moves to the central zone to promote both stem cell identity and *CLV3* expression (Yadav et al., 2011; Daum et al., 2014). The CLV3 ligand diffuses in the upper part of the meristem and triggers the CLV-CORYNE pathway that, together with RPK2, restricts *WUS* expression to the organizing center (Lenhard and Laux, 2003; Rojo et al., 2002; Kinoshita et al., 2010; Brand, 2000; Schoof et al., 2000; Müller et al., 2008). The *ERECTA* (*ER*) receptor kinase and most of the *HD-ZIPIII* genes have been shown to regulate meristem size and stem cell homeostasis through different pathways and in parallel to the CLV pathway (Green et al., 2005; Prigge et al., 2005; Williams, 2005; Mandel et al., 2014, 2016). All these genetic pathways, together with additional layers of control such as transcriptional regulators HAM (Zhou et al., 2018) and ULTRAPETALA1/2 (ULT1/2) (Carles, 2005; Monfared et al., 2013), chromatin regulators FAS1/2 (Kaya et al., 2001) and SYD (Kwon, 2005), cytokinins (Leibfried et al., 2005; Gordon et al., 2009), meristem geometry (Gruel et al., 2016) and environmental factors (Pfeiffer et al., 2017), robustly maintain and confine the stem cell niche before flowers are produced.

The flower initially inherits the potential of indeterminacy from the SAM: the maintenance of stem cells in the center of the flower relies on the same WUS/CLV regulatory loop (Schoof et al., 2000). Floral termination coincides with the end of *WUS* expression once carpels have been produced, at stage 6 (Smyth et al., 1990) in *A. thaliana* (Mayer et al., 1998). AGAMOUS (AG), a MADS box transcription factor (Yanofsky et al., 1990), is a key regulator in this process and triggers flower meristem termination by repressing *WUS* expression (Lohmann et al., 2001; Lenhard et al., 2001). This repression by AG can be direct, by recruiting polycomb group (PcG) factors and promoting a chromatin loop that blocks the recruitment of RNA polymerase II at the *WUS* locus (Liu et al., 2011; Guo et al., 2018), but also indirect through activation of KNUCKLES (KNU; a C2H2 Zn-finger transcription factor) (Sun et al., 2009). KNU is recruited to the *WUS* locus by MINI ZINC FINGER2 to form a complex together with HISTONE DEACETYLASE-like HDA19 and TOPLESS, which in turn inhibits *WUS* expression (Sun et al., 2009, 2014; Bollier et al., 2018). KNU also directly binds the *WUS* locus to cause eviction of SYD and subsequent recruitment of PcG factors to silence *WUS* (Sun et al., 2019). Consistently, most mutants showing flower termination defects also show a transient reduction in *AG* expression in the center of the flower (Clark et al., 1993; Fletcher, 2001; Prunet et al., 2008; Das et al., 2009; Maier et al., 2009). Interestingly, recent data report how AG also influences auxin and cytokinin biosynthesis during the flower meristem termination process (Yamaguchi et al., 2018; Zhang et al., 2018). Similarly, expression of a miR172-insentive version of *APETALA2* (*AP2*) results in a decrease in *AG* expression and in the development of supernumerary organs in the center of the flower (Zhao et al., 2007). AP2 may also promote floral stem cell maintenance by counteracting *AG* function (Zhao et al., 2007; Liu et al., 2014; Huang et al., 2017). Interestingly, mutations in many genes reported above as involved in the control of stem cell homeostasis in the SAM (including *CLV*, *ULT*, *ER*, *HD-ZipIII*) result in flower meristem indeterminacy, this phenotype often being related to a defect in *AG* expression. It seems, therefore, that *AG* expression is a good integrator and proxy for the final developmental decision to switch from an indeterminate to a determinate flower. Although single mutants have revealed that this process can be impaired, the contribution of transcriptional noise to the robustness of flower termination remains unknown.

We report here that mutations in Paf1c can result in loss of floral determinacy. Such a phenotype is caused by maintenance of stem cells in the center of the flower beyond stage 6, which results in a global decrease in *AG* expression in the center of the flower. Importantly, this phenotype is not fully penetrant, with flowers exhibiting subtle defects to fully indeterminate phenotypes, even on the same individual plant. This phenotype also depends on environmental conditions, suggesting that Paf1c integrates both developmental and environmental cues to reduce *AG* expression variability during flower development and to hinder floral indeterminacy.

RESULTS

vip3 mutants exhibit strong and variable flower indeterminacy

vip3 mutants have previously been reported to display a number of growth defects (Zhang et al., 2003; Takagi and Ueguchi, 2012; Dorcey et al., 2012; Fal et al., 2017). When *vip3* mutants were grown for 3 weeks under short day conditions (see Materials and Methods) at 21°C and then transferred to continuous light at 16°C, we observed a dramatic loss of floral indeterminacy such that, in some *vip3* plants, a wild-type sized inflorescence would grow out of a carpel (N>30 plants, Fig. 1A,B; Fig. S1). Whereas this phenotype was observed in both *vip3-1* and *vip3-2* alleles (Fig. 1C), silique development in the wild type remained entirely unaffected under these growth conditions (N>30 plants, Fig. 1A,C).

To check whether this phenotype depends on either the temperature or day length shift, we next studied the *vip3-1* phenotype under different growth conditions. Plants grown in continuous light but at 21°C instead of 16°C displayed a similar phenotype (N=32 plants, Fig. S2). We could also see the indeterminacy phenotype when *vip3-1* was constantly grown under short day conditions (N=9 plants, Fig. S3A) and under short then long day conditions (N=22 plants, Fig. S3B). When grown in long days, the *vip3* mutant was much smaller, with shorter stems, and exhibited a large number of aborted siliques without indeterminacy (N=36 plants, Fig. S3C). Therefore, floral termination defects in *vip3* only require short day conditions and no other specific growth conditions. Note that the *vip3* mutant was able to produce seeds but at a very low rate (Fig. S4), except when plants were grown exclusively under long day conditions that resulted in sterile siliques (Fig. S3C).

The extent of the floral indeterminacy defects in *vip3* depended on growth conditions: the *vip3* phenotype was most affected in short day and in short day then continuous light (16°C or 21°C) conditions and appeared to be the closest to a full reversal of floral identity, as reported in the literature. Note that we observed similar phenotypic defects in *vip6*, a mutant for another component of the Paf1 complex (N=19 plants, Fig. S3D). Such data further confirm that flower phenotypes result from defects in the Paf1-C and not in

Development (2019) 146, dev173377. doi:10.1242/dev.173377

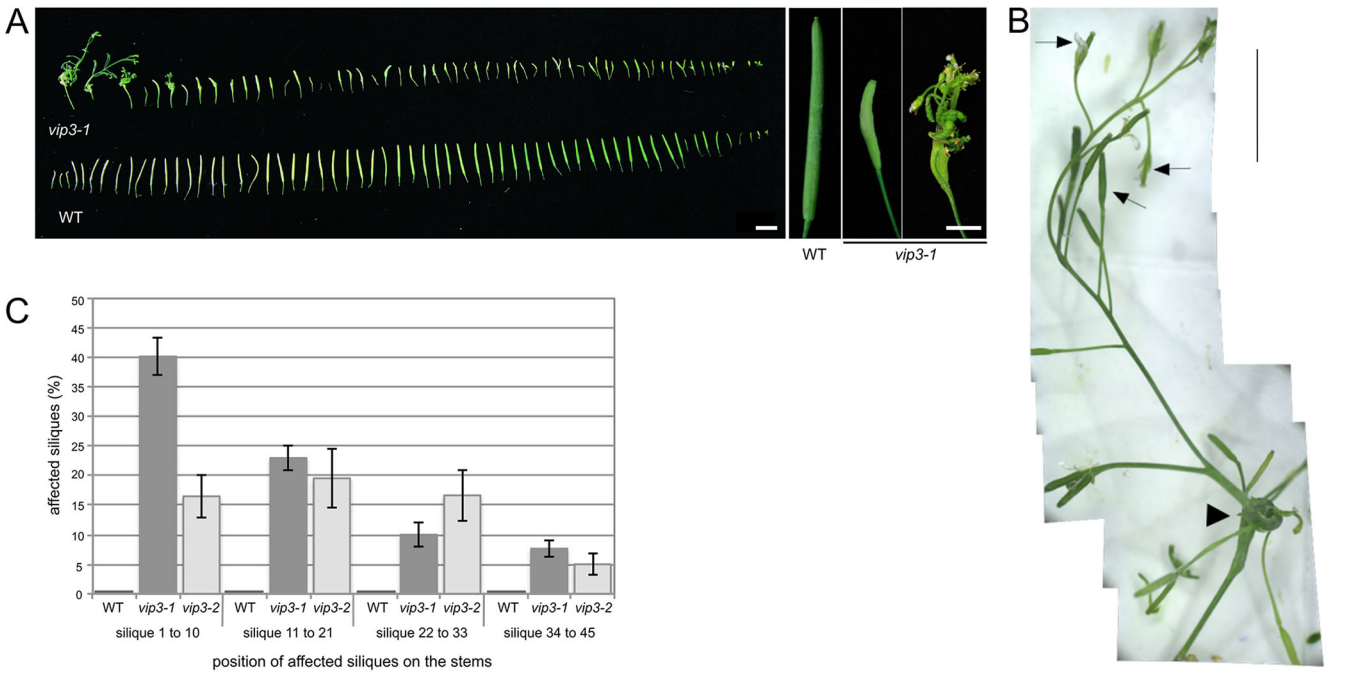

Fig. 1. *vip3* mutants can exhibit a severe flower indeterminacy phenotype. (A) Left: Representative phenotype of wild-type and *vip3* siliques, from plants grown in short day conditions at 21°C then continuous light at 16°C (*N*>30 plants), harvested from the stems in a sequence of initiation. Right: representative siliques of the wild type and *vip3* displaying different degrees of phenotypic defects. (B) Representative image of the most severe phenotype in *vip3-1* flowers. Arrowhead points at the primary silique; arrows point at secondary carpels. (C) Distribution (%) of affected siliques on the stems of the wild type (*N*=13), *vip3-1* (*N*=60) and *vip3-2* (*N*=20) grown in short day conditions at 21°C then continuous light at 16°C. On average, 20% of *vip3-1* and 14% of *vip3-2* siliques displayed visible indeterminacy defects in these conditions. Scale bars: 1 cm in A, left panel; 5 mm in A, right panel; 1 cm in B.

the exome complex, which is involved in mRNA turnover and which VIP3 (SKI8 analog), but not VIP6, is part of (Dorcey et al., 2012).

Furthermore, the *vip3* indeterminacy phenotype was also highly variable within a single plant (Fig. 1A; Fig. S2A). In comparison to the wild type, the phenotype ranged from short and bumpy siliques to completely open siliques containing a full inflorescence. With respect to the position of the siliques along the inflorescence stem, we found that early siliques were very often the most affected, although even the last siliques occasionally exhibited a strong phenotype (Fig. 1C; Fig. S2B).

Supernumerary organs develop from the center of the floral meristem

Except for branching meristems that develop from bract axils in species with a dichasium inflorescence (Claßen-Bockhoff and Bull-Hereñu, 2013) or from sepal axils in *ap1* mutants that lack petals and have sepals displaying bract-like features (Irish and Sussex, 1990; Mandel et al., 1992), there are two ways in which flower indeterminacy can occur: either the flower maintains its stem cells after stage 6 (Prunet et al., 2009) or ovules are homeotically converted into carpels (Modrusan et al., 1994; Pautot et al., 2001). In the latter case, one would expect to see multiple carpels growing within a single primary carpel. We never observed such a phenotype in *vip3* mutants; instead, the supernumerary organs all arose from the same stem or at least belonged to the same structure. It is therefore more likely that flower indeterminacy in *vip3* mutants is the result of a delay in flower termination. To confirm that hypothesis, we generated longitudinal sections through carpels in both wild-type and *vip3* carpels and stained the structures with toluidine blue. We observed that supernumerary organs always developed within the primary carpels on a stem emerging from the bottom of the flower (*N*=44 carpels, Fig. 2). We never detected supernumerary organs emerging from ovules. The presence of such long stems within the carpel has not been reported in other indeterminate mutants such as *crc ult*, *crc sqn*, *crc rbl*, *pwd*, *clv1* or *knu* (Prunet et al., 2008; Yumul et al., 2013; Clark et al., 1993; Sun et al., 2009).

RNA-seq analysis of *vip3-1* mutant shoot apices reveals genomewide expression defects

Given the strength of the phenotype, we first checked whether specific pathways are affected in *vip3*. To do so, we performed RNA-seq analyses of the *vip3-1* mutant, using shoot apices

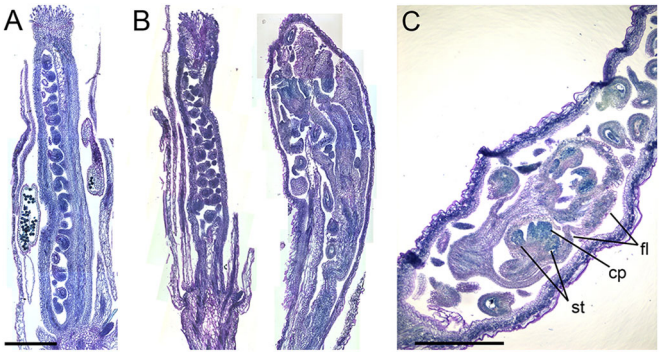

Fig. 2. Inflorescence stem and floral organs can be detected in *vip3* siliques. (A,B) Sections in young siliques, stained with toluidine blue. Wild-type (A) and representative *vip3* (B) siliques illustrate the spectrum of *vip3* phenotypes. (C) Section of young *vip3* silique, stained with Toluidine Blue, demonstrating the presence of floral structures inside the silique. cp, carpel; fl, flower; st, stamen. Scale bars: 500 µm.

Development (2019) 146, dev173377. doi:10.1242/dev.173377

(Fig. S5A,B). Note that this material only contained meristems and flowers up to stage 3 (i.e. not fully developed). The fold change for each gene was expressed in the log2 scale (meaning that a factor of 1 corresponds to a twofold change). This analysis revealed defects in *FLOWERING LOCUS C* (*FLC*) expression (downregulation by a factor 4.6; Fig. S5C), as already reported (Oh et al., 2008). However, this large-scale analysis did not reveal clear-cut defects in specific flowering pathways, but global defects in the transcriptome, even if we cannot exclude any defects on specific pathways due to statistical and/or detailed annotations limitations. Genes from the same family (e.g. MADS) displayed either reduced (e.g. *AGL31*, *AGL77*) or enhanced (e.g. *AGL71*) mRNA accumulation in *vip3-1* (Fig. S5C). A few putative regulators of *WUS*, such as *ULT2*, exhibited a significant decrease in mRNA accumulation (by a factor of 3.1), whereas *CLV3* mRNA accumulation was higher (by a factor of 2.4) in *vip3-1* (Fig. S5C). Other putative regulators such as *PHB*, *ERL1*, *HAM3* and *PAN* also show higher mRNA accumulations but with lower rates (by factors of 0.6, 0.8, 1 and 1.1, respectively; Fig. S5C). Similarly, we also found that hormone signaling pathways were affected, albeit without any clear-cut, specific trend. Yet, expression of genes involved in both auxin and cytokinin pathways seemed to be affected (Fig. S5D). Such data are consistent with previously reported phyllotactic defects in *vip3* (Fal et al., 2017) and with more recent data on hormonal control of floral determinacy (Yamaguchi et al., 2018; Zhang et al., 2018) as well as with the indeterminacy defects reported here. Note that RNA-seq data obtained previously on *vip3* seedlings also reflects such genomewide alteration, without clear-cut targets (Oh et al., 2008). Together, these data are consistent with the hypothesis that the *vip3* mutant does not affect specific pathways, but instead increases transcriptional noise, as assessed in yeast (Ansel et al., 2008). Ideally, single-cell RNA-seq analyses would provide quantitative data on transcriptional noise in plants. These results thus call for gene-by-gene analysis of expression patterns of specific regulators of stem cell maintenance and flower termination.

Development of supernumerary organs results from the prolonged maintenance of stem cells in the center of the flower

Because our phenotypic analysis suggested that the *vip3* indeterminacy phenotype was caused by prolonged maintenance of stem cells in flowers, we focused our analysis on the integrator of stem cell maintenance and flower termination, *WUS*. Using *in situ* hybridization, we observed a bright and localized signal in the organizing center of wild-type SAM and young flowers until stage 5 or 6 (N_{WT}=34 flowers; Fig. 3A) (Mayer et al., 1998). In *vip3*, we observed some flowers with a similar pattern, but others with more variable patterns. In particular, we detected *WUS* expression at the center of flowers at a much later stage than in the wild type (Fig. 3A; Fig. S6B), which is consistent with the indeterminacy phenotype. The *WUS* expression domain was also much broader than that of the wild type in certain *vip3* flowers ($N_{vip3\text{-}1}$=30 flowers, $N_{vip3\text{-}2}$=45 flowers; Fig. 3A; Fig. S6). To account for this variability in the spatial domain of *WUS* mRNA accumulation in *vip3*, we distinguished different types of patterns: the wild type displayed a single robust pattern, but the *vip3* mutant exhibited either a normal *WUS* expression domain (in 51 out of 73 meristems) or a larger and deeper *WUS* expression domain (in 22 out of 73 meristems; Fig. S6C). To further confirm these trends, we next analyzed the expression of *WUS* in a line expressing a fluorescent tag under the control of *WUS* promoter *pWUS::3xVENUS-N7* (Pfeiffer et al., 2016). The fluorescent pattern was wider in both wild-type and mutant flowers, as compared with our *in situ* hybridization data. Wider *pWUS::GFP* expression domains in the wild type have already been reported (Gordon et al., 2009). Nevertheless, we clearly observed an even wider expression of *WUS* in *vip3* flowers compared with wild-type flowers (N_{WT}=94 flowers, $N_{vip3\text{-}1}$=58 flowers; Fig. 4A). Quantification of the area of *WUS* expression revealed it to be up to two times larger in *vip3* than in the wild type (Fig. 4B). The coefficient of variation of *WUS* expression area was also significantly increased in *vip3* (Fig. S7A). Quantification of the average fluorescence intensity suggested a mild reduction in *WUS* promoter activity in *vip3*, although this might reflect a larger gradient domain (Fig. 4C). Based on both *in situ* hybridization data and fluorescent reporter lines, the *WUS* expression domain appeared variable and rather enlarged in *vip3*. As ectopic expression of *WUS* in flowers is also known to generate extra organs in the center of the flower (Lenhard et al., 2001), our data are consistent with the macroscopic indeterminacy phenotype in *vip3*. Note that we could not detect a significant effect of *vip3* mutation on the *CLV3* spatial expression domain by *in situ* hybridization. Yet, *CLV3* expression

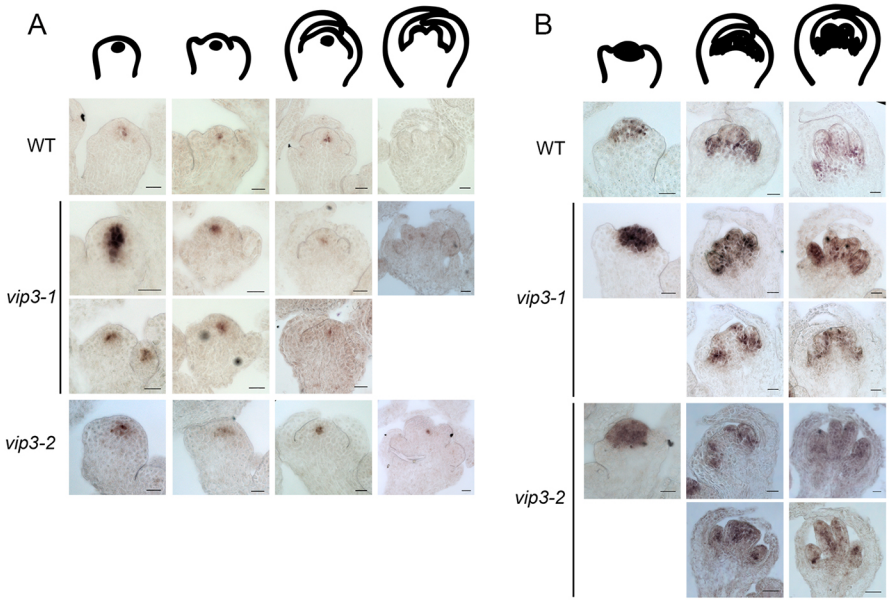

Fig. 3. Expression patterns of *WUS* and *AG* in *vip3* flowers. Representative *in situ* hybridization of (A) *WUS* (N_{WT}=34 flowers, $N_{vip3\text{-}1}$=30 flowers, $N_{vip3\text{-}2}$=45 flowers) and (B) *AG* (N_{WT}=33 flowers, $N_{vip3\text{-}1}$=35 flowers, $N_{vip3\text{-}2}$=12 flowers) transcripts in wild-type and *vip3* (*vip3-1* and *vip3-2*) flowers at four or three different developmental stages (as represented by the drawings). Plants for hybridization were grown in short day conditions at 21°C then continuous light at 16°C (as in Fig. 1). Scale bars: 20 µm.

Development (2019) 146, dev173377. doi:10.1242/dev.173377

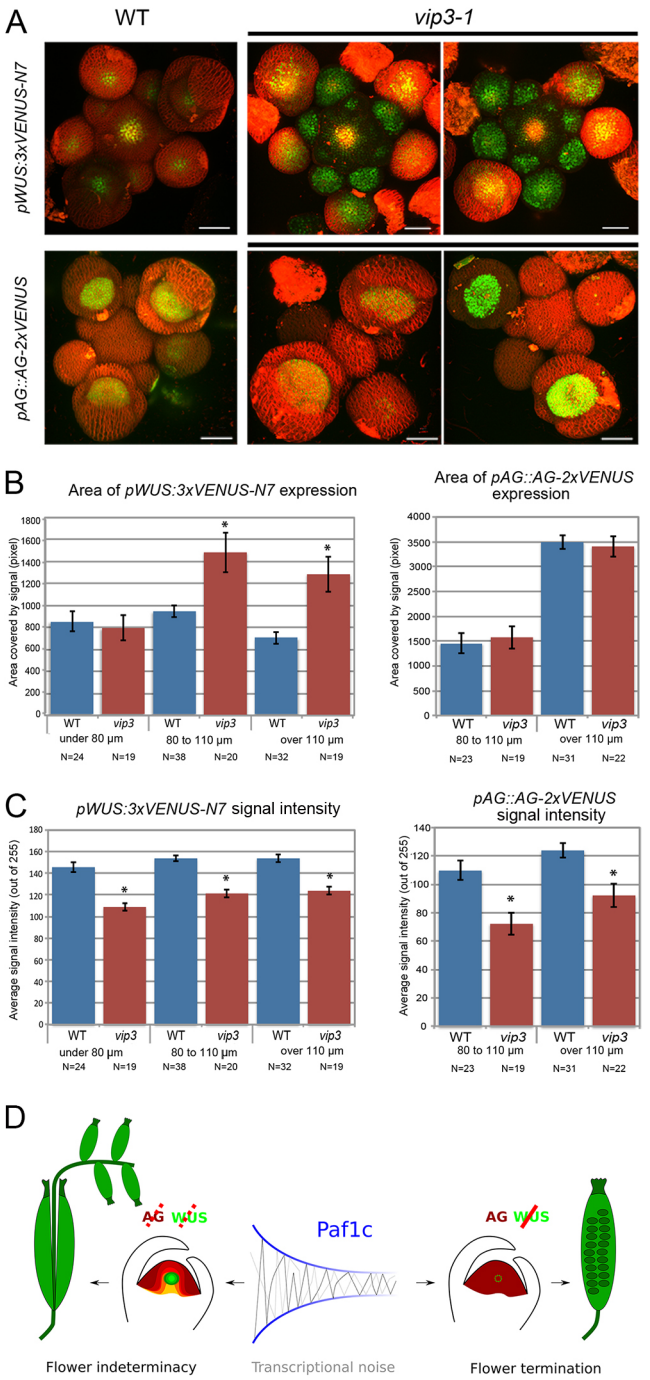

Fig. 4. Expression of *WUS* and *AG* reporter lines in *vip3* flowers. (A) Representative wild-type and *vip3-1* inflorescence meristems expressing *pWUS::3xVENUS-N7* (N_{WT}=94 flowers, $N_{vip3\text{-}1}$=58 flowers) and *pAG::AG-2xVENUS* (N_{WT}=54 flowers, $N_{vip3\text{-}1}$=41 flowers) reporters, labeled with FM4-64. (B) Area of *pWUS::3xVENUS-N7* (left) and *pAG::AG-2xVENUS* (right) expression in wild-type and *vip3-1* flowers of different size (<80, 80-110 and >110 µm). Flower diameter was calculated as described in Materials and Methods. (C) Average signal intensities (mean±s.e.m.) for *pWUS::3xVENUS-N7* (left) and *pAG::AG-2xVENUS* (right) in wild-type and *vip3-1* flowers of different size (<80, 80-110 and >110 µm). Results were considered significant when **P*<0.05% by the two-tailed Student's test. (D) VIP3 contributes to the robustness of flower meristem termination. Scale bars: 50 µm in A.

seemed to be maintained at later flower stages than in the wild type (in 6 out of 15 flower meristems beyond stage 6; N_{WT}=10 meristems, 12 flowers; $N_{vip3\text{-}1}$=9 meristems, 14 flowers; $N_{vip3\text{-}2}$=5 meristems, 5 flowers; Fig. S8). This is consistent with an overall delay in flower termination.

Mutation in *VIP3* results in a lower expression of AG in the center of the flower

Given that the *vip3* indeterminacy phenotype is strong and variable, and that it is associated with perturbed stem cell maintenance control, we analyzed expression of *AGAMOUS* (*AG*), the primary regulator of stem cell arrest in the flower. Analysis of the *AG* mRNA pattern through *in situ* hybridization revealed the expected pattern in the wild type, with strong accumulations in floral whorls 3 and 4, prior to the emergence of stamens and carpels (N_{WT}=33 flowers; Fig. 3B). Similar patterns were also observed in certain *vip3* flowers, but *AG* mRNA accumulation appeared much reduced in the center of whorl 4 in other flowers ($N_{vip3\text{-}1}$=35 flowers, $N_{vip3\text{-}2}$=12 flowers; Fig. 3B). To further confirm this result, we generated a fluorescently tagged version of AG under its own promoter (*pAG::AG-2xVenus*) and analyzed its expression profile. These data confirmed the results from the *in situ* hybridizations, and also showed a globally reduced level of AG in certain *vip3* flowers (N_{WT}=54 flowers, $N_{vip3\text{-}1}$=41 flowers; Fig. 4A,C). AG signal intensity was also more variable in *vip3* (Fig. S7B). The global area of AG expression was not significantly different in *vip3* and the wild type, consistent with the observations that the contours were not strongly affected and that only the center of flower exhibited defects in AG expression (Fig. 4B). Together, these results show that defects in Paf1c-dependent control of transcriptional noise lead to a delay in flower termination, notably through *AG* and *WUS* (Fig. 4D).

DISCUSSION

We have uncovered a strong floral indeterminacy phenotype in *vip3*. Flower development is usually considered to be highly robust in *A. thaliana*. Nonetheless, chimeric flowers can be produced at low frequency (Hempel and Feldman, 1995). Such flowers result from primordia exhibiting the features of both flowers and paraclades (lateral flowering shoot). Here, *vip3* flowers develop normally (in terms of identity) but a variable proportion do not stop producing organs beyond stage 6, resulting in short and bumpy siliques up to completely open siliques containing a full inflorescence. Most indeterminacy phenotypes reported so far result in the production of extra floral organs, mostly carpels and stamens, rarely petals except in strong *ag* mutants that reiterate complete flowers (Bowman et al., 1989; Prunet et al., 2009). Thus, in mutants with weaker phenotypes than that of *vip3*, floral meristem identity is never, or extremely rarely, lost. The only cases where a full new inflorescence was reported is in *clv1-4* flowers where, in rare cases, a new inflorescence with developing flowers emerges from the gynoecium (Clark et al., 1993). Although this new inflorescence is obtained through gain of function, the *p35S::XAL2* line, in which the MADS box transcription factor XAL2/AGL14 is overexpressed, also displays major indeterminacy defects that resemble those of *vip3* mutants (Pérez-Ruiz et al., 2015). Our results in *vip3* mutants suggest that full reversion might be reachable through a more global perturbation of transcription. This calls for a more systemic investigation of the molecular players behind floral indeterminacy. In fact, these results also question the limits of the reductionist approach: genetic screens for floral indeterminacy did not uncover the *vip3* mutant, either because growth conditions were not appropriate or because variable phenotypes are less likely to be identified and selected.

Early stages of growth in short day conditions appeared essential to trigger the indeterminacy phenotype in *vip3*. This is consistent

Development (2019) 146, dev173377. doi:10.1242/dev.173377

with the reported role of the Paf1 complex in the regulation of flowering time and *FLC* expression (Zhang et al., 2003). The results also reveal that a late phenotype (carpel differentiation) depends on very early cues during development. Our findings thus suggest that floral indeterminacy is much more plastic than anticipated, integrating the larger plant status early in development. The indeterminacy defects are not detected in long day conditions, but are observed in short day or continuous light conditions. Given that the latter growth conditions enhance meristem size (Landrein et al., 2015), it is possible that a threshold in meristem size is required for the indeterminacy phenotype to exist. In this respect, cytokinins are likely to play a strong integrator role, given their known impact on the regulation of *WUS* expression and meristem size (Pfeiffer et al., 2016; Landrein et al., 2018). Beyond cytokinins, the larger hormonal network is probably involved. For instance, in our RNA-seq analysis, we also found that YUC4, a target of AG and CRC (Yamaguchi et al., 2018), was downregulated in *vip3-1*. It remains to be shown whether such conclusions apply to other species; data in Impatiens balsamina suggest that it is the case (Pouteau et al., 1997).

As *AG* is deregulated in *vip3* mutants, our study also introduces Paf1c as a new player in the flower termination pathway. The use of lines expressing the antisense *AG* RNA gave a range of phenotypes, spanning from a weak indeterminacy phenotype (normal flower with few extra organs developing inside the primary carpels) to the canonical *ag* phenotype ([sepals-petals-petals]*n*), each category corresponding to a lower level of endogenous *AG* expression (Mizukami and Ma, 1995). In *vip3*, we observed weaker AG expression in the floral domain that corresponds to the fourth whorl subdomain that develops carpel margins and placenta. The reduced AG level in *vip3* might be consistent with the reported increase in H3K27me3 over the *AG* region in the mutant (see figure S4 in Oh et al., 2008). Our study thus opens the possibility that part of the plasticity in carpel development relies on Paf1c-dependent *AG* expression.

Our results echo the rising role of incomplete penetrance in developmental plasticity. Incomplete penetrance is intrinsically caused by random fluctuations in gene expression (Raj and van Oudenaarden, 2008). Such variability contributes to cell fate specification in multicellular organisms (Chang et al., 2008; Hume, 2000; Wernet et al., 2006). The existence of such variability could lead to incoherencies in gene networks; yet it can also provide a way for the network to become less sensitive to environmental fluctuations. In other words, cells can still retain the ability to acquire alternative fates, despite the channeling effect of environmental cues (Hart et al., 2014). Interestingly, we find that the *vip3* indeterminacy phenotype occurs when *WUS* expression slowly decreases in wild-type flowers. Gene expression fading (in and out) and low levels of gene expression might represent weak points in gene networks, as variability in gene expression (area, intensity and duration) in such instances can have more pronounced effects. Conversely, the gene regulatory network often promotes clear-cut expression patterns (both in space and time) and this could limit the presence of such weak points. It appears surprising that a developmental switch as important as the decision to stop or maintain stem cells in a flower relies on such a robust Boolean control, yet our results in the *vip3* mutant suggest that increased transcriptional noise is sufficient to induce indeterminacy. This calls for an analysis of the adaptive benefits of such a weak control. One could speculate that the number of fruits and seeds would be increased via this unusual prolongation of floral stem cell competence, as observed in other species (Tooke et al., 2005).

MATERIALS AND METHODS

Plant lines

All procedures were performed on plants from the Col-0 ecotype. The *pWUS::3xVENUS-N7* reporter lines (Pfeiffer et al., 2016) and T-DNA insertion lines *vip3-1* (salk139885) and *vip3-2* (salk083364) were used for this study (genotyping primers are listed in Table S1). To generate the *pAG::AG-2xVenus* line, we used a fragment of genomic *AG* from Col-0, containing 2655 bp of upstream sequence, the 1061 bp 5′UTR (which includes intron 1) and 4241 bp from start to stop (which includes the 2999 bp second intron), amplified with the pPD381 and pPD413 primers (see Table S1) and transferred with *Xma*I digestion in BJ36 containing 2xVenus fluorescent reporter. BJ36 with 2xVenus was obtained from pCS2-Venus with pPD441 and pPD442 primers (see Table S1) adding 5xAla at the beginning of Venus and transferred twice in BJ36 through *Bam*HI and *Xma*I digestion. The *pAG::AG-2xVenus* obtained fragment was transferred in *pART* (a kanamycin-resistant vector) with *Xma*I digestion and then transformed in Col-0 plants using *Agrobacterium tumefaciens*.

Growth conditions

In ‘short day’ conditions, plants were grown under a 8 h (21°C)/16 h (15°C) light/dark period. In ‘long day’ conditions, plants were grown under a 16 h (21°C)/8 h (19°C) light/dark period. In continuous light conditions, plants were grown under continuous light at 16°C or 21°C. In ‘short day then long day or continuous light conditions’, plants were first grown for 3 weeks in short day conditions and then transferred to long day or continuous light conditions.

RNA-seq analysis of *vip3* shoot apices

vip3-1 and Col-0 shoot apices (from plants grown in short day conditions at 21°C then continuous light at 16°C) were dissected by removing flowers older than stage 4. Samples were collected into liquid nitrogen-cooled Eppendorf tubes directly after dissection, each tube containing between 30 and 35 apices, 6 samples for each genotype. RNA extraction was performed using the PicoPure RNA Isolation Kit Arcturus (ThermoFisher, KIT0204) with an on-column DNase treatment (Qiagen, catalog#79254). After elution, two samples were combined together, obtaining the final technical triplicates for each genotype. RNA concentrations in the samples were measured by Bioanalyser (Plant RNA Nano Assay, Agilent Technologies, Chip priming station number 5065-4401, 16-pin bayonet electrode cartridge, order number 5065-4413) and sent for sequencing. Total RNA libraries preparation, Illumina sequencing and initial data analysis were performed by Fasteris (HiSeq instrument, Basecalling pipeline, HiSeq Control Software HD 3.4.0.38, analysed with Expression_mRNA_tuxedo). Adapter trimming was with Trimmomatic, a flexible read trimming tool for Illumina NGS data (Bolger et al., 2014). Mapping was with BOWTIE 2.0.5 (Langmead et al., 2009), TOPHAT 2.0.6 (tophat.cbcb.umd.edu/) and SAMTOOLS 1.2 (www.htslib.org/). The reference genome was *Arabidopsis thaliana* Ensembly TAIR10, from iGenome. Expression estimation, normalization and comparison was carried out using CUFFLINKS v2.1.1 (cufflinks.cbcb.umd.edu/).

Histological sections and *in situ* hybridization

The *in situ* hybridization on paraplast-embedded tissues was performed as described (Vernoux et al., 2011). Shoot apices were sectioned into slices 8 µm thick. The probes for the coding regions of *WUS* and *AG* were amplified with specific primers (listed in Table S1), where the T7 promoter sequence was added to the reverse primer. PCR products were further purified with the QIAquick PCR Purification Kit (Qiagen ID 28106). *In vitro* transcription and DIG labeling of the probes were performed with the T7 RNA polymerase (Promega, P2077) and DIG RNA Labeling Mix (Roche 11277073910). For histological sections, late flowers (stage 15-16) were harvested and paraplast-embedded following the same protocol. After sectioning, paraffin removal and rehydration, the samples were stained with 0.1% toluidine blue solution. Images were acquired using the Zeiss Imager.M2 microscope (20× and 40× objectives) and the Axiocam 503. Results were obtained in triplicates (three independent rounds of *in situ* hybridizations, from independently grown plant populations).

Confocal laser scanning microscopy and image analysis

Dissected meristems and plants grown *in vitro* were imaged with a water dipping lens (25×, NA=0.8) using a SP8 confocal microscope (Leica, Germany) to generate a stack of optical sections with an interval of 0.2 µm between slices. The membranes were stained with FM4-64. Image analysis was performed using the Fiji software (fiji.sc/wiki/index.php/Fiji). The fluorescence intensity and size of the fluorescent area were extracted from the maximum projections of the image stacks of each individual flowers using the ROI tool. For smaller flowers, about 280 slices were imaged, representing a stack 56 µm thick; for older flowers, about 430 slices were imaged, representing a stack 87 µm thick. Average diameter of the flowers was calculated by tracing four lines between the edges of a flower, crossing in the center with a 45° angle between each pair of lines. The extracted ROI values were further analyzed using Microsoft Excel. Statistical analysis was performed using either Microsoft Excel or R softwares. The two-tailed Student's test was used to compare means of independent biological replicates. Results were obtained in triplicates (three independent rounds of imaging sessions, from independently grown plant populations).

Acknowledgements

We thank Toshiro Ito for constructive discussions about this project and our colleagues for critical reading of the manuscript. We also thank Platim for help with imaging, and Jérémy Just for help with RNA-seq data processing and submission. We acknowledge Jan Lohmann for providing the *pWUS::3xVENUS-N7* reporter line. We also thank the anonymous reviewers for their constructive comments.

Competing interests

The authors declare no competing or financial interests.

Author contributions

Conceptualization: K.F., O.H., C.T.; Methodology: K.F., M.C., M.L.; Validation: K.F., M.C.; Formal analysis: K.F., M.C.; Investigation: K.F., M.C.; Resources: M.L., S.C., P.D.; Data curation: K.F., M.C.; Writing - original draft: O.H.; Writing - review & editing: K.F., P.D., C.T.; Visualization: K.F., M.C.; Supervision: K.F., P.D., O.H., C.T.; Project administration: O.H., C.T.; Funding acquisition: O.H.

Funding

This work was supported by the European Research Council (615739), by 'MechanoDevo', by the Fondation Schlumberger pour l'Education et la Recherche and by Association Nationale de la Recherche et de la Technologie (CIFRE contract 2017/0975). Deposited in PMC for immediate release.

Data availability

RNA-seq data have been deposited in Gene Expression Omnibus under accession number GSE139201.

Supplementary information

Supplementary information available online at
http://dev.biologists.org/lookup/doi/10.1242/dev.173377.supplemental

References

Alemu, E. Y., Carl, J. W., Corrada Bravo, H. and Hannenhalli, S. (2014). Determinants of expression variability. *Nucleic Acids Res.* **42**, 3503-3514. doi:10.1093/nar/gkt1364

Ansel, J., Bottin, H., Rodriguez-Beltran, C., Damon, C., Nagarajan, M., Fehrmann, S., François, J. and Yvert, G. (2008). Cell-to-cell stochastic variation in gene expression is a complex genetic trait. *PLoS Genet.* **4**, e1000049. doi:10.1371/journal.pgen.1000049

Antosz, W., Pfab, A., Ehrnsberger, H. F., Holzinger, P., Köllen, K., Mortensen, S. A., Bruckmann, A., Schubert, T., Längst, G., Griesenbeck, J. et al. (2017). The composition of the arabidopsis RNA polymerase II transcript elongation complex reveals the interplay between elongation and mRNA processing factors. *Plant Cell* **29**, 854-870. doi:10.1105/tpc.16.00735

Besnard, F., Vernoux, T. and Hamant, O. (2011). Organogenesis from stem cells in planta: multiple feedback loops integrating molecular and mechanical signals. *Cell. Mol. Life Sci.* **68**, 2885-2906. doi:10.1007/s00018-011-0732-4

Bolger, A. M., Lohse, M. and Usadel, B. (2014). Trimmomatic: a flexible trimmer for illumina sequence data. *Bioinformatics* **30**, 2114-2120. doi: 10.1093/bioinformatics/btu170

Bollier, N., Sicard, A., Leblond, J., Latrasse, D., Gonzalez, N., Gévaudant, F., Benhamed, M., Raynaud, C., Lenhard, M., Chevalier, C. et al. (2018). At-mini zinc finger2 and SL-inhibitor of meristem activity, a conserved missing link in the regulation of floral meristem termination in arabidopsis and tomato. *Plant Cell* **30**, 83-100. doi:10.1105/tpc.17.00653

Bowman, J. L., Smyth, D. R. and Meyerowitz, E. M. (1989). Genes directing flower development in Arabidopsis. *Plant Cell* **1**, 37-52. doi:10.1105/tpc.1.1.37

Brand, U. (2000). Dependence of stem cell fate in arabidopsis on a feedback loop regulated by CLV3 activity. *Science* **289**, 617-619. doi:10.1126/science.289.5479.617

Carles, C. C. (2005). ULTRAPETALA1 encodes a SAND domain putative transcriptional regulator that controls shoot and floral meristem activity in Arabidopsis. *Development* **132**, 897-911. doi:10.1242/dev.01642

Chang, H. H., Hemberg, M., Barahona, M., Ingber, D. E. and Huang, S. (2008). Transcriptome-wide noise controls lineage choice in mammalian progenitor cells. *Nature* **453**, 544-547. doi:10.1038/nature06965

Chen, F. X., Xie, P., Collings, C. K., Cao, K., Aoi, Y., Marshall, S. A., Rendleman, E. J., Ugarenko, M., Ozark, P. A., Zhang, A. et al. (2017). PAF1 regulation of promoter-proximal pause release via enhancer activation. *Science* **357**, 1294-1298. doi:10.1126/science.aan3269

Clark, S. E., Running, M. P. and Meyerowitz, E. M. (1993). CLAVATA1, a regulator of meristem and flower development in Arabidopsis. *Development* **119**, 397-418.

Claßen-Bockhoff, R. and Bull-Hereñu, K. (2013). Towards an ontogenetic understanding of inflorescence diversity. *Ann. Bot.* **112**, 1523-1542. doi:10.1093/aob/mct009

Das, P., Ito, T., Wellmer, F., Vernoux, T., Dedieu, A., Traas, J. and Meyerowitz, E. M. (2009). Floral stem cell termination involves the direct regulation of AGAMOUS by PERIANTHIA. *Development* **136**, 1605-1611. doi:10.1242/dev.035436

Daum, G., Medzihradszky, A., Suzaki, T. and Lohmann, J. U. (2014). A mechanistic framework for noncell autonomous stem cell induction in Arabidopsis. *Proc. Natl. Acad. Sci. USA* **111**, 14619-14624. doi:10.1073/pnas.1406446111

Dorcey, E., Rodriguez-Villalon, A., Salinas, P., Santuari, L., Pradervand, S., Harshman, K. and Hardtke, C. S. (2012). Context-dependent dual role of SKI8 homologs in mRNA synthesis and turnover. *PLoS Genet.* **8**, e1002652. doi:10.1371/journal.pgen.1002652

Fal, K., Liu, M., Duisembekova, A., Refahi, Y., Haswell, E. S. and Hamant, O. (2017). Phyllotactic regularity requires the Paf1 complex in Arabidopsis. *Development* **144**, 4428-4436. doi:10.1242/dev.154369

Fletcher, J. C. (2001). The ULTRAPETALA gene controls shoot and floral meristem size in Arabidopsis. *Development* **128**, 1323-1333.

Gordon, S. P., Chickarmane, V. S., Ohno, C. and Meyerowitz, E. M. (2009). Multiple feedback loops through cytokinin signaling control stem cell number within the Arabidopsis shoot meristem. *Proc. Natl. Acad. Sci. USA* **106**, 16529-16534. doi:10.1073/pnas.0908122106

Green, K. A., Prigge, M. J., Katzman, R. B. and Clark, S. E. (2005). *CORONA*, a member of the class III homeodomain leucine zipper gene family in arabidopsis, regulates stem cell specification and organogenesis. *Plant Cell* **17**, 691-704. doi:10.1105/tpc.104.026179

Gruel, J., Landrein, B., Tarr, P., Schuster, C., Refahi, Y., Sampathkumar, A., Hamant, O., Meyerowitz, E. M. and Jönsson, H. (2016). An epidermis-driven mechanism positions and scales stem cell niches in plants. *Sci. Adv.* **2**, e1500989. doi:10.1126/sciadv.1500989

Guo, L., Cao, X., Liu, Y., Li, J., Li, Y., Li, D., Zhang, K., Gao, C., Dong, A. and Liu, X. (2018). A chromatin loop represses *WUSCHEL* expression in Arabidopsis. *Plant J.* **94**, 1083-1097. doi:10.1111/tpj.13921

Hamant, O., Das, P. and Burian, A. (2014). Time-lapse imaging of developing meristems using confocal laser scanning microscope. *Methods Mol. Biol.* **1080**, 111-119. doi:10.1007/978-1-62703-643-6_9

Hart, Y., Reich-Zeliger, S., Antebi, Y. E., Zaretsky, I., Mayo, A. E., Alon, U. and Friedman, N. (2014). Paradoxical signaling by a secreted molecule leads to homeostasis of cell levels. *Cell* **158**, 1022-1032. doi:10.1016/j.cell.2014.07.033

He, Y., Doyle, M. R. and Amasino, R. M. (2004). PAF1-complex-mediated histone methylation of FLOWERING LOCUS C chromatin is required for the vernalization-responsive, winter-annual habit in Arabidopsis. *Genes Dev.* **18**, 2774-2784. doi:10.1101/gad.1244504

Hempel, F. D. and Feldman, L. J. (1995). Specification of chimeric flowering shoots in wild-type Arabidopsis. *Plant J.* **8**, 725-731. doi:10.1046/j.1365-313X.1995.08050725.x

Huang, Z., Shi, T., Zheng, B., Yumul, R. E., Liu, X., You, C., Gao, Z., Xiao, L. and Chen, X. (2017). *APETALA2* antagonizes the transcriptional activity of *AGAMOUS* in regulating floral stem cells in *Arabidopsis thaliana*. *New Phytol.* **215**, 1197-1209. doi:10.1111/nph.14151

Hume, D. A. (2000). Probability in transcriptional regulation and its implications for leukocyte differentiation and inducible gene expression. *Blood* **96**, 2323-2328.

Irish, V. F. and Sussex, I. M. (1990). Function of the apetala-1 gene during Arabidopsis floral development. *Plant Cell* **2**, 741-753. doi:10.1105/tpc.2.8.741

Kaya, H., Shibahara, K.-I., Taoka, K.-I., Iwabuchi, M., Stillman, B. and Araki, T. (2001). FASCIATA genes for chromatin assembly factor-1 in arabidopsis maintain the cellular organization of apical meristems. *Cell* **104**, 131-142. doi:10.1016/S0092-8674(01)00197-0

Kinoshita, A., Betsuyaku, S., Osakabe, Y., Mizuno, S., Nagawa, S., Stahl, Y., Simon, R., Yamaguchi-Shinozaki, K., Fukuda, H. and Sawa, S. (2010). RPK2 is an essential receptor-like kinase that transmits the CLV3 signal in Arabidopsis. *Development* **137**, 3911-3920. doi:10.1242/dev.048199

Kwon, C. S. (2005). WUSCHEL is a primary target for transcriptional regulation by SPLAYED in dynamic control of stem cell fate in Arabidopsis. *Genes Dev.* **19**, 992-1003. doi:10.1101/gad.1276305

Landrein, B., Refahi, Y., Besnard, F., Hervieux, N., Mirabet, V., Boudaoud, A., Vernoux, T. and Hamant, O. (2015). Meristem size contributes to the robustness of phyllotaxis in Arabidopsis. *J. Exp. Bot.* **66**, 1317-1324. doi: 10.1093/jxb/eru482.

Landrein, B., Formosa-Jordan, P., Malivert, A., Schuster, C., Melnyk, C. W., Yang, W., Turnbull, C., Meyerowitz, E. M., Locke, J. C. W. and Jönsson, H. (2018). Nitrate modulates stem cell dynamics in Arabidopsis shoot meristems through cytokinins. *Proc. Natl. Acad. Sci. USA* **115**, 1382-1387. doi:10.1073/pnas.1718670115

Langmead, B., Trapnell, C., Pop, M. and Salzberg, S. L. (2009). Ultrafast and memory-efficient alignment of short DNA sequences to the human genome. *Genome Biol.* **10**, R25. doi:10.1186/gb-2009-10-3-r25

Leibfried, A., To, J. P. C., Busch, W., Stehling, S., Kehle, A., Demar, M., Kieber, J. J. and Lohmann, J. U. (2005). WUSCHEL controls meristem function by direct regulation of cytokinin-inducible response regulators. *Nature* **438**, 1172-1175. doi:10.1038/nature04270

Lenhard, M. and Laux, T. (2003). Stem cell homeostasis in the Arabidopsis shoot meristem is regulated by intercellular movement of CLAVATA3 and its sequestration by CLAVATA1. *Development* **130**, 3163-3173. doi:10.1242/dev.00525

Lenhard, M., Bohnert, A., Jürgens, G. and Laux, T. (2001). Termination of stem cell maintenance in Arabidopsis floral meristems by interactions between WUSCHEL and AGAMOUS. *Cell* **105**, 805-814. doi:10.1016/S0092-8674(01)00390-7

Liu, X., Kim, Y. J., Müller, R., Yumul, R. E., Liu, C., Pan, Y., Cao, X., Goodrich, J. and Chen, X. (2011). AGAMOUS terminates floral stem cell maintenance in arabidopsis by directly repressing WUSCHEL through recruitment of Polycomb group proteins. *Plant Cell* **23**, 3654-3670. doi:10.1105/tpc.111.091538

Liu, X., Dinh, T. T., Li, D., Shi, B., Li, Y., Cao, X., Guo, L., Pan, Y., Jiao, Y. and Chen, X. (2014). *AUXIN RESPONSE FACTOR 3* integrates the functions of *AGAMOUS* and *APETALA2* in floral meristem determinacy. *The Plant Journal* **80**, 629-641. doi:10.1111/tpj.12658

Lohmann, J. U., Hong, R. L., Hobe, M., Busch, M. A., Parcy, F., Simon, R. and Weigel, D. (2001). A molecular link between stem cell regulation and floral patterning in Arabidopsis. *Cell* **105**, 793-803. doi:10.1016/S0092-8674(01)00384-1

Maier, A. T., Stehling-Sun, S., Wollmann, H., Demar, M., Hong, R. L., Haubeiss, S., Weigel, D. and Lohmann, J. U. (2009). Dual roles of the bZIP transcription factor PERIANTHIA in the control of floral architecture and homeotic gene expression. *Development* **136**, 1613-1620. doi:10.1242/dev.033647

Mandel, M. A., Gustafson-Brown, C., Savidge, B. and Yanofsky, M. F. (1992). Molecular characterization of the Arabidopsis floral homeotic gene APETALA1. *Nature* **360**, 273-277. doi:10.1038/360273a0

Mandel, T., Moreau, F., Kutsher, Y., Fletcher, J. C., Carles, C. C. and Williams, L. E. (2014). The ERECTA receptor kinase regulates Arabidopsis shoot apical meristem size, phyllotaxy and floral meristem identity. *Development* **141**, 830-841. doi:10.1242/dev.104687

Mandel, T., Candela, H., Landau, U., Asis, L., Zelinger, E., Carles, C. C. and Williams, L. E. (2016). Differential regulation of meristem size, morphology and organization by the ERECTA, CLAVATA and class III HD-ZIP pathways. *Development* **143**, 1612-1622. doi:10.1242/dev.129973

Mantsoki, A., Devailly, G. and Joshi, A. (2016). Gene expression variability in mammalian embryonic stem cells using single cell RNA-seq data. *Comput. Biol. Chem.* **63**, 52-61. doi:10.1016/j.compbiolchem.2016.02.004

Mason, E. A., Mar, J. C., Laslett, A. L., Pera, M. F., Quackenbush, J., Wolvetang, E. and Wells, C. A. (2014). Gene expression variability as a unifying element of the pluripotency network. *Stem Cell Rep.* **3**, 365-377. doi:10.1016/j.stemcr.2014.06.008

Mayer, K. F. X., Schoof, H., Haecker, A., Lenhard, M., Jürgens, G. and Laux, T. (1998). Role of WUSCHEL in regulating stem cell fate in the Arabidopsis shoot meristem. *Cell* **95**, 805-815. doi:10.1016/S0092-8674(00)81703-1

Meyer, H. M., Teles, J., Formosa-Jordan, P., Refahi, Y., San-Bento, R., Ingram, G., Jönsson, H., Locke, J. C. W. and Roeder, A. H. K. (2017). Fluctuations of the transcription factor ATML1 generate the pattern of giant cells in the Arabidopsis sepal. *eLife* **6**, e19131. doi:10.7554/eLife.19131

Mizukami, Y. and Ma, H. (1995). Separation of AG function in floral meristem determinacy from that in reproductive organ identity by expressing antisense AG RNA. *Plant Mol. Biol.* **28**, 767-784. doi:10.1007/BF00042064

Modrusan, Z., Reiser, L., Feldmann, K. A., Fischer, R. L. and Haughn, G. W. (1994). Homeotic transformation of ovules into carpel-like structures in arabidopsis. *Plant Cell* **6**, 333-349. doi:10.2307/3869754

Momiji, H. and Monk, N. A. M. (2009). Oscillatory Notch-pathway activity in a delay model of neuronal differentiation. *Phys. Rev. E Stat. Nonlin. Soft Matter Phys.* **80**, 021930. doi:10.1103/PhysRevE.80.021930

Monfared, M. M., Carles, C. C., Rossignol, P., Pires, H. R. and Fletcher, J. C. (2013). The ULT1 and ULT2 trxG genes play overlapping roles in Arabidopsis development and gene regulation. *Mol. Plant* **6**, 1564-1579. doi:10.1093/mp/sst041

Müller, R., Bleckmann, A. and Simon, R. (2008). The receptor kinase CORYNE of arabidopsis transmits the stem cell-limiting signal CLAVATA3 independently of CLAVATA1. *Plant Cell Online* **20**, 934-946. doi:10.1105/tpc.107.057547

Oh, S., Zhang, H., Ludwig, P. and van Nocker, S. (2004). A mechanism related to the yeast transcriptional regulator Paf1c is required for expression of the Arabidopsis FLC/MAF MADS box gene family. *Plant Cell* **16**, 2940-2953. doi:10.1105/tpc.104.026062

Oh, S., Park, S. and van Nocker, S. (2008). Genic and global functions for Paf1C in chromatin modification and gene expression in Arabidopsis. *PLoS Genet.* **4**, e1000077. doi:10.1371/journal.pgen.1000077

Padovan-Merhar, O. and Raj, A. (2013). Using variability in gene expression as a tool for studying gene regulation: characterizing gene regulation using expression variability. *Wiley Interdiscip. Rev. Syst. Biol. Med.* **5**, 751-759. doi:10.1002/wsbm.1243

Pautot, V., Dockx, J., Hamant, O., Kronenberger, J., Grandjean, O., Jublot, D. and Traas, J. (2001). KNAT2: evidence for a link between knotted-like genes and carpel development. *Plant Cell* **13**, 1719-1734. doi:10.1105/TPC.010184

Pérez-Ruiz, R. V., García-Ponce, B., Marsch-Martínez, N., Ugartechea-Chirino, Y., Villajuana-Bonequi, M., de Folter, S., Azpeitia, E., Dávila-Velderrain, J., Cruz-Sánchez, D., Garay-Arroyo, A. et al. (2015). XAANTAL2 (AGL14) is an important component of the complex gene regulatory network that underlies arabidopsis shoot apical meristem transitions. *Mol. Plant* **8**, 796-813. doi:10.1016/j.molp.2015.01.017

Pfeiffer, A., Janocha, D., Dong, Y., Medzihradszky, A., Schöne, S., Daum, G., Suzaki, T., Forner, J., Langenecker, T., Rempel, E. et al. (2016). Integration of light and metabolic signals for stem cell activation at the shoot apical meristem. *eLife* **5**, e17023. doi:10.7554/eLife.17023

Pfeiffer, A., Wenzl, C. and Lohmann, J. U. (2017). Beyond flexibility: controlling stem cells in an ever changing environment. *Curr. Opin. Plant Biol.* **35**, 117-123. doi:10.1016/j.pbi.2016.11.014

Pouteau, S., Nicholls, D., Tooke, F., Coen, E. and Battey, N. (1997). The induction and maintenance of flowering in Impatiens. *Development* **124**, 3343-3351.

Prigge, M. J., Otsuga, D., Alonso, J. M., Ecker, J. R., Drews, G. N. and Clark, S. E. (2005). Class III homeodomain-leucine zipper gene family members have overlapping, antagonistic, and distinct roles in arabidopsis development. *Plant Cell* **17**, 61-76. doi:10.1105/tpc.104.026161

Prunet, N., Morel, P., Thierry, A.-M., Eshed, Y., Bowman, J. L., Negrutiu, I. and Trehin, C. (2008). REBELOTE, SQUINT, and ULTRAPETALA1 function redundantly in the temporal regulation of floral meristem termination in Arabidopsis thaliana. *Plant Cell Online* **20**, 901-919. doi:10.1105/tpc.107.053306

Prunet, N., Morel, P., Negrutiu, I. and Trehin, C. (2009). Time to stop: flower meristem termination. *Plant Physiol.* **150**, 1764-1772. doi:10.1104/pp.109.141812

Raj, A. and van Oudenaarden, A. (2008). Nature, nurture, or chance: stochastic gene expression and its consequences. *Cell* **135**, 216-226. doi:10.1016/j.cell.2008.09.050

Raj, A., Rifkin, S. A., Andersen, E. and van Oudenaarden, A. (2010). Variability in gene expression underlies incomplete penetrance. *Nature* **463**, 913-918. doi:10.1038/nature08781

Richard, M. and Yvert, G. (2014). How does evolution tune biological noise? *Front. Genet.* **5**, 374. doi:10.3389/fgene.2014.00374

Rojo, E., Sharma, V. K., Kovaleva, V., Raikhel, N. V. and Fletcher, J. C. (2002). CLV3 is localized to the extracellular space, where it activates the Arabidopsis CLAVATA stem cell signaling pathway. *Plant Cell Online* **14**, 969-977. doi:10.1105/tpc.002196

Schoof, H., Lenhard, M., Haecker, A., Mayer, K. F. X., Jürgens, G. and Laux, T. (2000). The stem cell population of Arabidopsis shoot meristems is maintained by a regulatory loop between the CLAVATA and WUSCHEL genes. *Cell* **100**, 635-644. doi:10.1016/S0092-8674(00)80700-X

Smyth, D. R., Bowman, J. L. and Meyerowitz, E. M. (1990). Early flower development in Arabidopsis. *Plant Cell* **2**, 755-767. doi:10.1105/tpc.2.8.755

Somssich, M., Je, B. I., Simon, R. and Jackson, D. (2016). CLAVATA-WUSCHEL signaling in the shoot meristem. *Development* **143**, 3238-3248. doi:10.1242/dev.133645

Sprinzak, D., Lakhanpal, A., LeBon, L., Santat, L. A., Fontes, M. E., Anderson, G. A., Garcia-Ojalvo, J. and Elowitz, M. B. (2010). Cis-interactions between Notch and Delta generate mutually exclusive signalling states. *Nature* **465**, 86-90. doi:10.1038/nature08959

Sun, B., Xu, Y., Ng, K.-H. and Ito, T. (2009). A timing mechanism for stem cell maintenance and differentiation in the Arabidopsis floral meristem. *Genes Dev.* **23**, 1791-1804. doi:10.1101/gad.1800409

Sun, B., Looi, L.-S., Guo, S., He, Z., Gan, E.-S., Huang, J., Xu, Y., Wee, W.-Y. and Ito, T. (2014). Timing mechanism dependent on cell division is invoked by polycomb eviction in plant stem cells. *Science* **343**, 1248559-1248559. doi:10.1126/science.1248559

Sun, B., Zhou, Y., Cai, J., Shang, E., Yamaguchi, N., Xiao, J., Looi, L.-S., Wee, W.-Y., Gao, X., Wagner, D. et al. (2019). Integration of transcriptional repression and polycomb-mediated silencing of *WUSCHEL* in floral meristems. *Plant Cell* **31**, 1488-1505. doi:10.1105/tpc.18.00450

Takagi, N. and Ueguchi, C. (2012). Enhancement of meristem formation by bouquet-1, a mis-sense allele of the vernalization independence 3 gene encoding a WD40 repeat protein in Arabidopsis thaliana. *Genes Cells* **17**, 982-993. doi:10.1111/gtc.12014

Tooke, F., Ordidge, M., Chiurugwi, T. and Battey, N. (2005). Mechanisms and function of flower and inflorescence reversion. *J. Exp. Bot.* **56**, 2587-2599. doi:10.1093/jxb/eri254

Tsugawa, S., Hervieux, N., Kierzkowski, D., Routier-Kierzkowska, A.-L., Sapala, A., Hamant, O., Smith, R. S., Roeder, A. H. K., Boudaoud, A. and Li, C.-B. (2017). Clones of cells switch from reduction to enhancement of size variability in Arabidopsis sepals. *Development* **144**, 4398-4405. doi:10.1242/dev.153999

Vernoux, T., Brunoud, G., Farcot, E., Morin, V., Van den Daele, H., Legrand, J., Oliva, M., Das, P., Larrieu, A., Wells, D. et al. (2011). The auxin signalling network translates dynamic input into robust patterning at the shoot apex. *Mol. Syst. Biol.* **7**, 508. doi:10.1038/msb.2011.39

Wang, J., Liu, D., Guo, X., Yang, W., Wang, X., Zhan, K. and Zhang, A. (2011). Variability of gene expression after polyhaploidization in wheat (*Triticum aestivum* L.). *G3* **1**, 27-33. doi:10.1534/g3.111.000091

Waters, A. J., Makarevitch, I., Noshay, J., Burghardt, L. T., Hirsch, C. N., Hirsch, C. D. and Springer, N. M. (2017). Natural variation for gene expression responses to abiotic stress in maize. *Plant J.* **89**, 706-717. doi:10.1111/tpj.13414

Wernet, M. F., Mazzoni, E. O., Çelik, A., Duncan, D. M., Duncan, I. and Desplan, C. (2006). Stochastic spineless expression creates the retinal mosaic for colour vision. *Nature* **440**, 174-180. doi:10.1038/nature04615

Williams, L. (2005). Regulation of Arabidopsis shoot apical meristem and lateral organ formation by microRNA miR166g and its AtHD-ZIP target genes. *Development* **132**, 3657-3668. doi:10.1242/dev.01942

Xu, Q., Zhu, C., Fan, Y., Song, Z., Xing, S., Liu, W., Yan, J. and Sang, T. (2016). Population transcriptomics uncovers the regulation of gene expression variation in adaptation to changing environment. *Sci. Rep.* **6**, 25536. doi:10.1038/srep25536

Yadav, R. K., Perales, M., Gruel, J., Girke, T., Jönsson, H. and Reddy, G. V. (2011). WUSCHEL protein movement mediates stem cell homeostasis in the Arabidopsis shoot apex. *Genes Dev.* **25**, 2025-2030. doi:10.1101/gad.17258511

Yamaguchi, N., Huang, J., Tatsumi, Y., Abe, M., Sugano, S. S., Kojima, M., Takebayashi, Y., Kiba, T., Yokoyama, R., Nishitani, K. et al. (2018). Chromatin-mediated feed-forward auxin biosynthesis in floral meristem determinacy. *Nat. Commun.* **9**, 5290. doi:10.1038/s41467-018-07763-0

Yanofsky, M. F., Ma, H., Bowman, J. L., Drews, G. N., Feldmann, K. A. and Meyerowitz, E. M. (1990). The protein encoded by the Arabidopsis homeotic gene agamous resembles transcription factors. *Nature* **346**, 35-39. doi:10.1038/346035a0

Yumul, R. E., Kim, Y. J., Liu, X., Wang, R., Ding, J., Xiao, L. and Chen, X. (2013). POWERDRESS and diversified expression of the MIR172 gene family bolster the floral stem cell network. *PLoS Genet.* **9**, e1003218. doi:10.1371/journal.pgen.1003218

Zhang, H., Ransom, C., Ludwig, P. and van Nocker, S. (2003). Genetic analysis of early flowering mutants in Arabidopsis defines a class of pleiotropic developmental regulator required for expression of the flowering-time switch flowering locus C. *Genetics* **164**, 347-358.

Zhang, K., Wang, R., Zi, H., Li, Y., Cao, X., Li, D., Guo, L., Tong, J., Pan, Y., Jiao, Y. et al. (2018). Auxin response FACTOR3 regulates floral meristem determinacy by repressing cytokinin biosynthesis and signaling. *Plant Cell* **30**, 324-346. doi:10.1105/tpc.17.00705

Zhao, L., Kim, Y. J., Dinh, T. T. and Chen, X. (2007). miR172 regulates stem cell fate and defines the inner boundary of APETALA3 and PISTILLATA expression domain in Arabidopsis floral meristems. *Plant J.* **51**, 840-849. doi:10.1111/j.1365-313X.2007.03181.x

Zhou, Y., Yan, A., Han, H., Li, T., Geng, Y., Liu, X. and Meyerowitz, E. M. (2018). HAIRY MERISTEM with WUSCHEL confines CLAVATA3 expression to the outer apical meristem layers. *Science* **361**, 502-506. doi:10.1126/science.aar8638

Summary: Using a mutant with increased transcriptional noise, we reveal that stem cell maintenance is not as robust as anticipated in plants, even leading to major defects in essential developmental processes such as flower indeterminacy.

Funding details

S.No.	Funder name	Funder ID	Grant ID
1	European Research Council	http://dx.doi.org/10.13039/100010663	
2	Fondation Schlumberger pour l'Education et la Recherche		
3	Association Nationale de la Recherche et de la Technologie	http://dx.doi.org/10.13039/501100003032	2017/0975

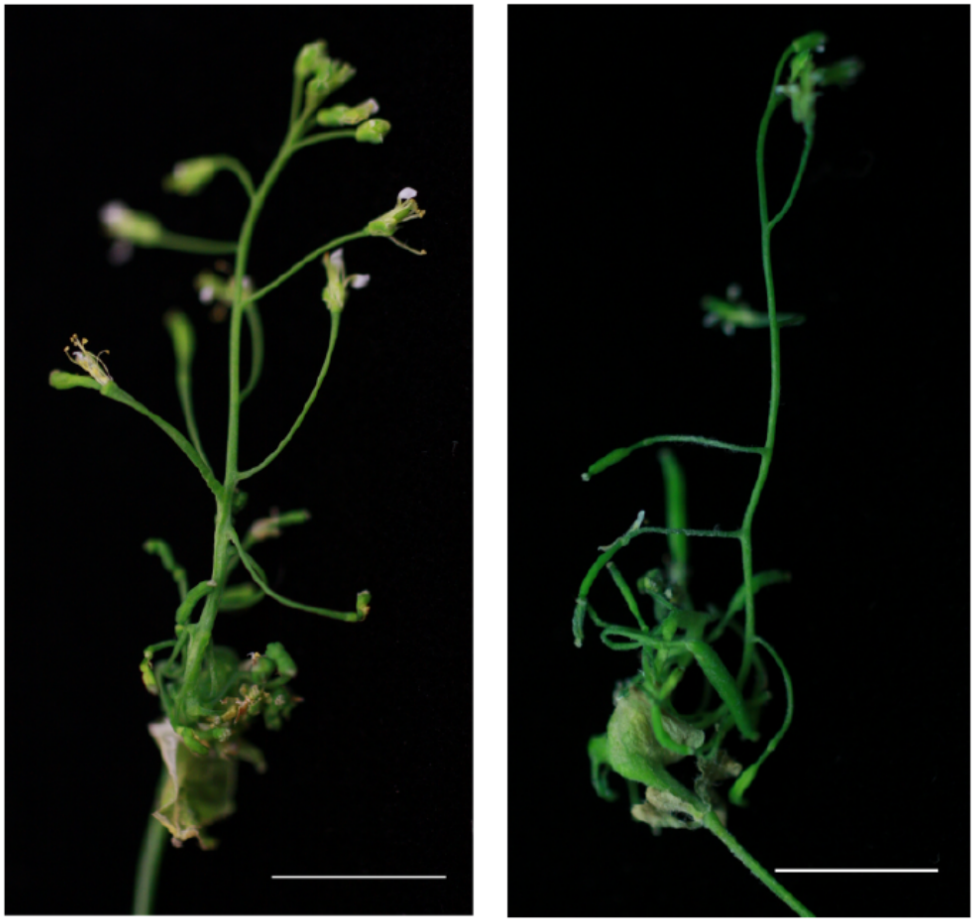

Fig. S1. Examples of the most severe indeterminacy phenotypes in *vip3-1* siliques.
Representative images of the most severe phenotypes in *vip3-1* flowers, displaying an inflorescence stem with siliques and flowers, emerging from a silique. Scale bar: 1 cm.

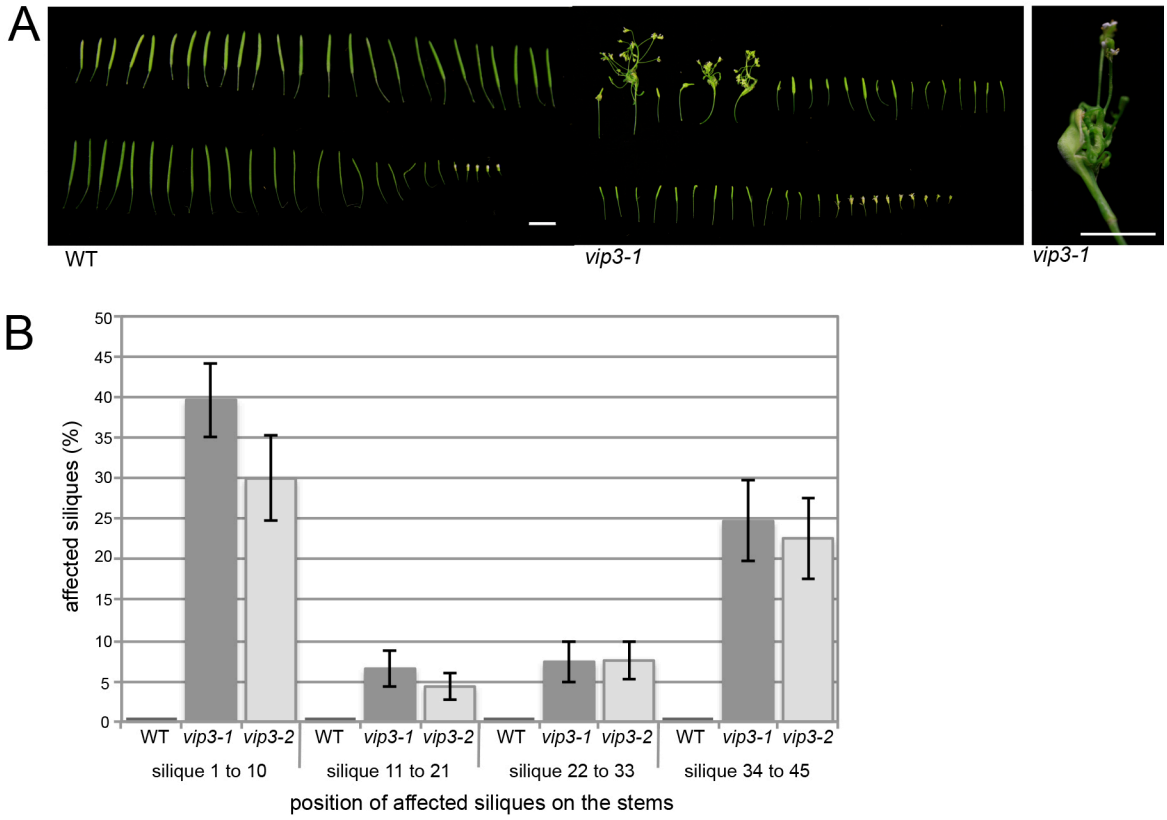

Fig. S2. *vip3* phenotype in short day then continuous light 21°C.

(A) Phenotype of WT (left panel) and *vip3-1* (middle panel) siliques, from plants grown in short day 21°C followed by continuous light 21°C conditions, harvested in a sequence of initiation along the stem. Scale bar : 1 cm. Right panel shows representative silique of the *vip3* displaying the indeterminacy phenotype. Scale bar : 5 mm. (B) Distribution (%) of affected siliques along the stems of the wild type (N=13), *vip3-1* (N=32) and *vip3-2* (N=21) grown in short day 21°C followed by continuous light 21°C condition (on average, 19% of *vip3-1* and 17% of *vip3-2* siliques displayed visible indeterminacy defects in these conditions).

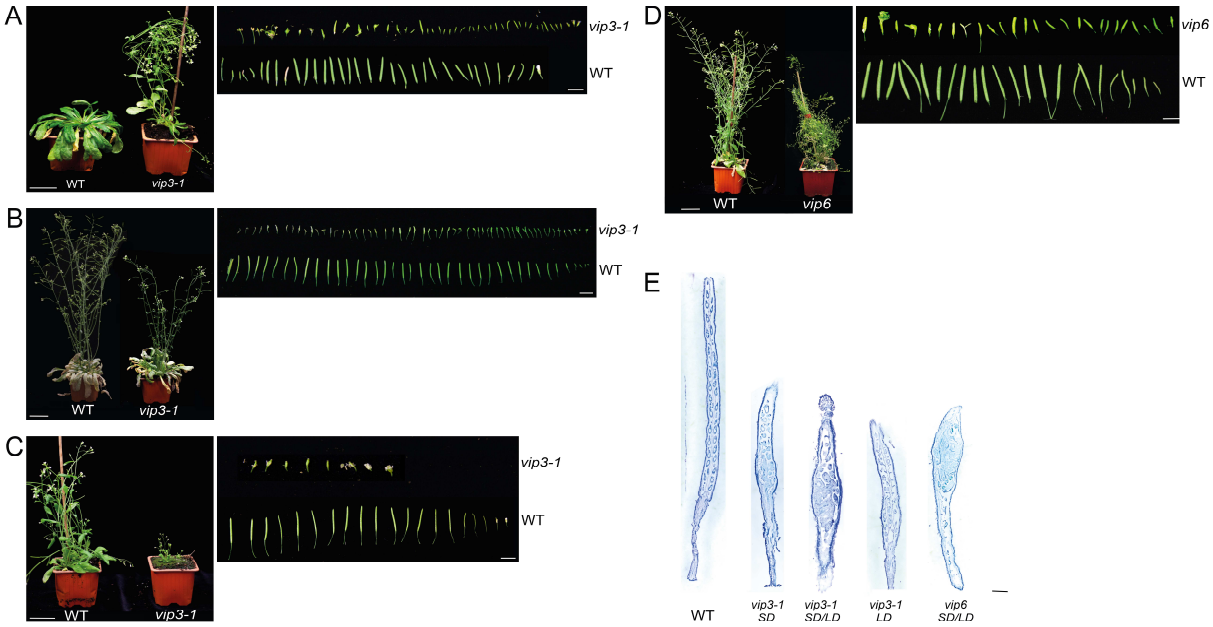

Fig. S3. Indeterminacy phenotype in different growth conditions and in different mutants of the Paf1 complex.

(A-C) Phenotypes of WT and *vip3-1* mutants grown in short day conditions (A, N=9 plants), in short then long day conditions (B, N=22 plants), and in long day conditions (C, N=22 plants). (D) Phenotype of WT and *vip6* mutant grown in short day 21°C followed by continuous light 16°C conditions displaying the indeterminacy phenotype (N=19 plants). For each condition, left panels display wild-type and *vip* adult plants, and right panels the siliques harvested in the order of their initiation along the stem. (E) Representative sections in young siliques, stained with toluidine blue, of *vip3-1*, in each culture condition, and *vip6* mutant, displaying the indeterminacy phenotype. Scale bars : 3 cm (A-D, left panels); 1 cm (A-D, right panels); 500 µm (E).

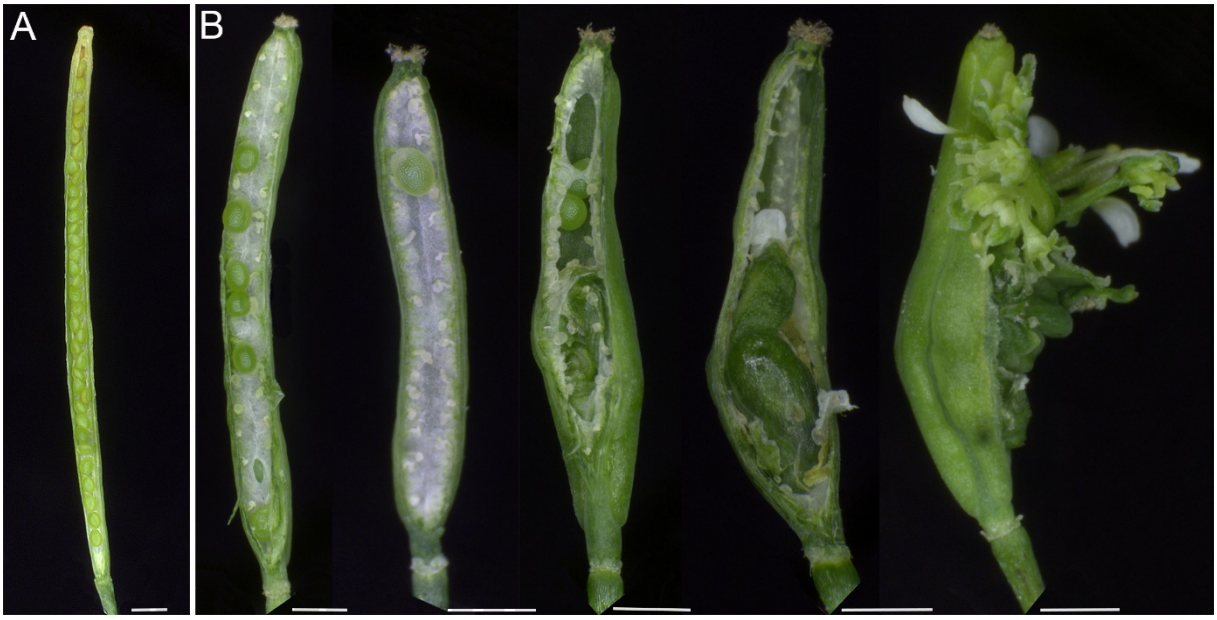

C	Number of ovules per silique		Number of aborted ovules per silique		Number of fertilized ovules per silique	
	WT	vip3-1	WT	vip3-1	WT	vip3-1
Mean	69,4	74,3	2,8	19,7	64,6	6,1
Standard deviation	3,9	18,2	0,9	11	3,7	6,8
Standard error of the mean	0,5	2,1	0,1	1,3	0,4	0,8
% compare to the total number of ovules per silique	-	-	4	26,5	93,1	8,2

Fig. S4. Proportion of aborted ovules and seeds in *vip3-1*.

(A-B) illustrates the range of phenotypes observed in *vip3-1* (B) compared to Col0 (A) (grown in short day and then in continuous light 16°C). *vip3-1* displays a strong and highly variable reduction of seed set in siliques showing no indeterminacy. In silique showing indeterminacy no or very few seeds usually develop. Bars = 500 µm. (C) Number of aborted ovules and seeds in *vip3-1* (N=73 siliques) and WT (N=70 siliques). The standard deviation reflects the variability of the original distribution. The standard error of the mean indicates the precision of estimated means (95% confidence interval).

A

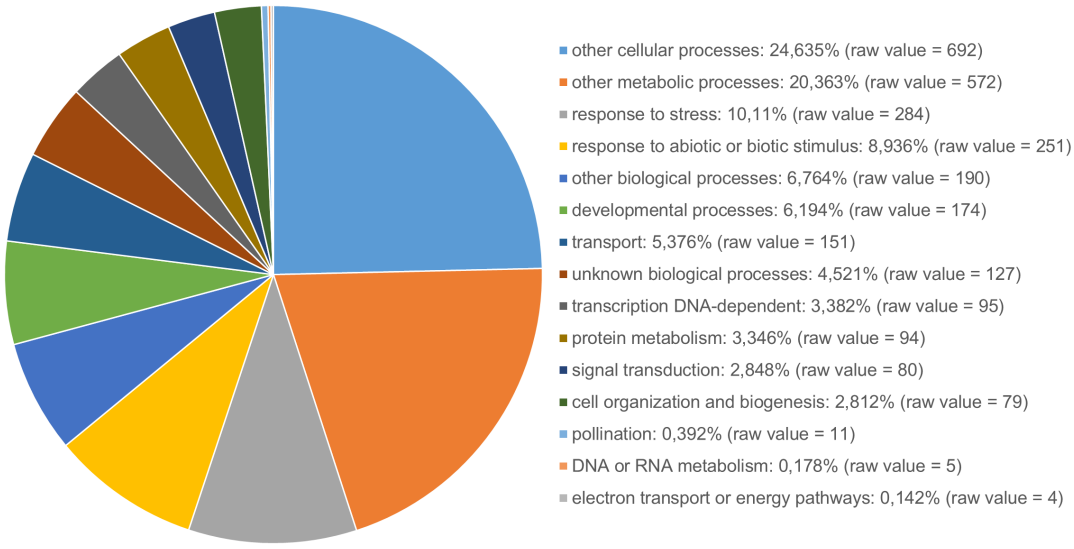

B

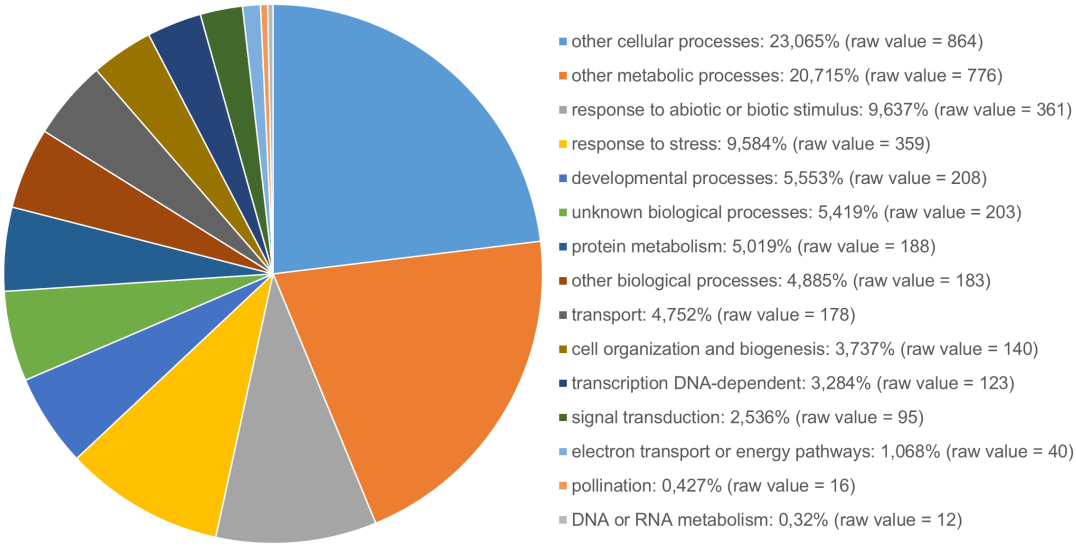

C

	gene_id	gene	log2(fold_change)	p_value
Downregulated	AT1G77080	FLM, FLOWERING LOCUS M / MAF1, MADS AFFECTING FLOWERING 1	-8,89394	5,00E-05
	AT5G65060	FCL3, FLOWERING LOCUS 3 / MAF3, MADS AFFECTING FLOWERING 3	-8,38456	0,0018
	AT5G10140	FLC, FLOWERING LOCUS C	-4,65699	5,00E-05
	AT5G65080	AGL68, AGAMOUS-LIKE 68 / MAF5, MADS AFFECTING FLOWERING 5	-4,15656	5,00E-05
	AT5G65050	AGL31, AGAMOUS-LIKE 31 / MAF2, MADS AFFECTING FLOWERING 2	-3,93607	5,00E-05
	AT5G38740	AGL77, AGAMOUS-LIKE 77	-3,33443	5,00E-05
	AT2G20825	ULT2, ULTRAPETALA2	-3,10298	5,00E-05
	AT5G27580	AGL89, AGAMOUS-LIKE 89	-2,67671	0,00405
	AT4G24540	AGL24, AGAMOUS-LIKE 24	-2,29325	5,00E-05
	AT4G27330	NZZ, NOZZLE / SPL, SPOROCYTELESS	-1,86166	0,00155
	AT5G60440	AGL62, AGAMOUS-LIKE 62	-1,59424	0,00795
	AT5G21150	AGO9, ARGONAUTE 9	-1,2134	5,00E-05
	AT5G57390	AIL5, AINTEGUMENTA-LIKE 5 / CHO1, CHOTTO 1 / EMK, EMBRYOMAKER / PLT5, PLETHORA 5	-0,866008	5,00E-05
	AT2G03060	AGL30, AGAMOUS-LIKE 30	-0,794353	0,001
	AT2G26440	PME12, PECTIN METHYLESTERASE 12	-0,709637	5,00E-05
Upregulated	AT3G20810	JMJ30 / JMJD5, JUMONJI DOMAIN CONTAINING 5	0,505522	0,00085
	AT4G37650	SGR7, SHOOT GRAVITROPISM 7 / SHR, SHORT ROOT	0,507952	0,00035
	AT2G33880	WOX9, WUSCHEL-RELATED HOMEOBOX 9	0,571996	0,00045
	AT2G34710	PHB, PHABULOSA / ATHB-14, ARABIDOPSIS THALIANA HOMEOBOX PROTEIN 14	0,586075	5,00E-05
	AT1G62360	STM, SHOOTMERISTEMLESS	0,589834	0,0001
	AT1G19850	MP, MONOPTEROS / ARF5, AUXIN RESPONSE FACTOR 5	0,608684	0,0019
	AT3G11050	FER2,- FERRITIN 2	0,652661	0,0039
	AT1G69770	CMT3, CHROMOMETHYLASE 3	0,707429	5,00E-05
	AT4G20270	BAM3, BARELY ANY MERISTEM 3	0,779995	5,00E-05
	AT5G62230	ERL1, ERECTA-LIKE 1	0,835578	5,00E-05
	AT5G53950	CUC2, CUP-SHAPED COTYLEDON 2	0,910426	5,00E-05
	AT5G11320	YUC4, YUCCA4	1,05308	5,00E-05
	AT2G45660	SOC1, SUPPRESSOR OF OVEREXPRESSION OF CO 1	1,0598	5,00E-05
	AT4G00150	HAM3, HAIRY MERISTEM 3, ATHAM3, HAIRY MERISTEM 3, HAM3, LOM3, LOST MERISTEMS 3, SCL6-IV	1,08428	5,00E-05
	AT1G68640	PAN; PERIANTHIA, TGA8, TGACG SEQUENCE-SPECIFIC BINDING PROTEIN 8	1,10476	5,00E-05
	AT3G15400	ATA20, ANTHER 20	2,05576	5,00E-05
	AT2G27250	CLV3, CLAVATA3	2,39061	5,00E-05
	AT1G75940	ATA27, BETA GLUCOSIDASE 20, BGLU20	2,50951	5,00E-05
	AT5G51870	AGL71, AGAMOUS-LIKE 71	2,85072	5,00E-05
	AT4G28395	ATA7, ARABIDOPSIS THALIANA ANTHER 7	3,11384	5,00E-05

D

	gene_id	gene	log2(fold_change)	p_value
Downregulated	AT2G14610	PR1; pathogenesis-related protein 1	-5,18392	5,00E-05
	AT5G59220	HAI1; PP2C protein (Clade A protein phosphatases type 2C)	-1,72227	5,00E-05
	AT4G34760	SAUR-like auxin-responsive protein family	-1,13968	5,00E-05
	AT1G08320	TGA9; bZIP transcription factor family protein	-0,969944	0,00355
	AT1G67710	ARR11; response regulator 11	-0,934393	0,00065
	AT3G23030	IAA2; indole-3-acetic acid inducible 2	-0,884945	0,0009
	AT4G34000	ABF3; abscisic acid responsive elements-binding factor 3	-0,857165	5,00E-05
	AT5G54510	DFL1; Auxin-responsive GH3 family protein	-0,799458	5,00E-05
	AT5G57560	TCH4; Xyloglucan endotransglucosylase/hydrolase family protein	-0,672642	5,00E-05
	AT3G23050	IAA7; indole-3-acetic acid 7	-0,628497	0,00325
	AT1G03430	AHP5; histidine-containing phosphotransfer factor 5	-0,590316	0,0007
	AT4G34750	SAUR-like auxin-responsive protein family	-0,579414	0,00535
Upregulated	AT1G80100	AHP6; histidine phosphotransfer protein 6	0,514231	0,0006
	AT2G22670	IAA8; indoleacetic acid-induced protein 8	0,537947	0,00075
	AT3G63010	GID1B; alpha/beta-Hydrolases superfamily protein	0,572849	0,00025
	AT1G28130	GH3.17; Auxin-responsive GH3 family protein	0,575311	5,00E-05
	AT5G46570	BSK2; BR-signaling kinase 2	0,576718	5,00E-05
	AT1G19850	MP; Transcriptional factor B3 family protein / auxin-responsive factor AUX/IAA-like protein	0,608684	0,0019
	AT1G51950	IAA18; indole-3-acetic acid inducible 18	0,628133	5,00E-05
	AT5G46790	PYL1; PYR1-like 1	0,646811	5,00E-05
	AT2G38120	AUX1; Transmembrane amino acid transporter family protein	0,691917	5,00E-05
	AT2G01570	RGA1; GRAS family transcription factor family protein	0,759926	5,00E-05
	AT1G45249	ABF2; abscisic acid responsive elements-binding factor 2	0,794846	5,00E-05
	AT1G19050	ARR7; response regulator 7	0,811842	5,00E-05
	AT2G38310	PYL4; PYR1-like 4	0,856148	5,00E-05
	AT4G27260	WES1; Auxin-responsive GH3 family protein	0,864813	5,00E-05
	AT1G72450	JAZ6; jasmonate-zim-domain protein 6	0,885443	5,00E-05
	AT1G17380	JAZ5; jasmonate-zim-domain protein 5	0,960683	5,00E-05
	AT4G33950	OST1; Protein kinase superfamily protein	1,02011	5,00E-05
	AT5G13220	JAZ10; jasmonate-zim-domain protein 10	1,03421	5,00E-05
	AT1G19180	JAZ1; jasmonate-zim-domain protein 1	1,04499	5,00E-05
	AT5G11320	YUC4, YUCCA4	1,05308	5,00E-05
	AT2G41310	RR3; response regulator 3	1,11732	5,00E-05
	AT1G77920	TGA7; bZIP transcription factor family protein	1,15091	0,00385
	AT5G17490	RGL3; RGA-like protein 3	1,15216	5,00E-05
	AT3G11410	PP2CA; protein phosphatase 2CA	1,21844	5,00E-05
	AT4G14550	IAA14; indole-3-acetic acid inducible 14	1,31153	0,0009
	AT1G04250	AXR3; AUX/IAA transcriptional regulator family protein	1,58048	0,0001
	AT3G21510	AHP1; histidine-containing phosphotransmitter 1	1,80767	0,00015
	AT1G77690	LAX3; like AUX1 3	2,1705	5,00E-05
	AT4G00880	SAUR-like auxin-responsive protein family	2,62316	5,00E-05
	AT5G13380	Auxin-responsive GH3 family protein	3,54665	5,00E-05
	AT2G46690	SAUR-like auxin-responsive protein family	3,63345	5,00E-05

Fig. S5. Differential gene expression in *vip3-1* vs. wild-type shoot apices.

(A, B) Gene ontology analysis: categories of genes involved in biological processes that are up-regulated (A) and down-regulated (B) in *vip3-1*. (C, D) Short list of genes involved in flowering and flower development (C) and signaling (D) pathways that are misexpressed in *vip3-1*. Genes that are down-regulated are highlighted in blue, and those that are up-regulated are highlighted in orange.

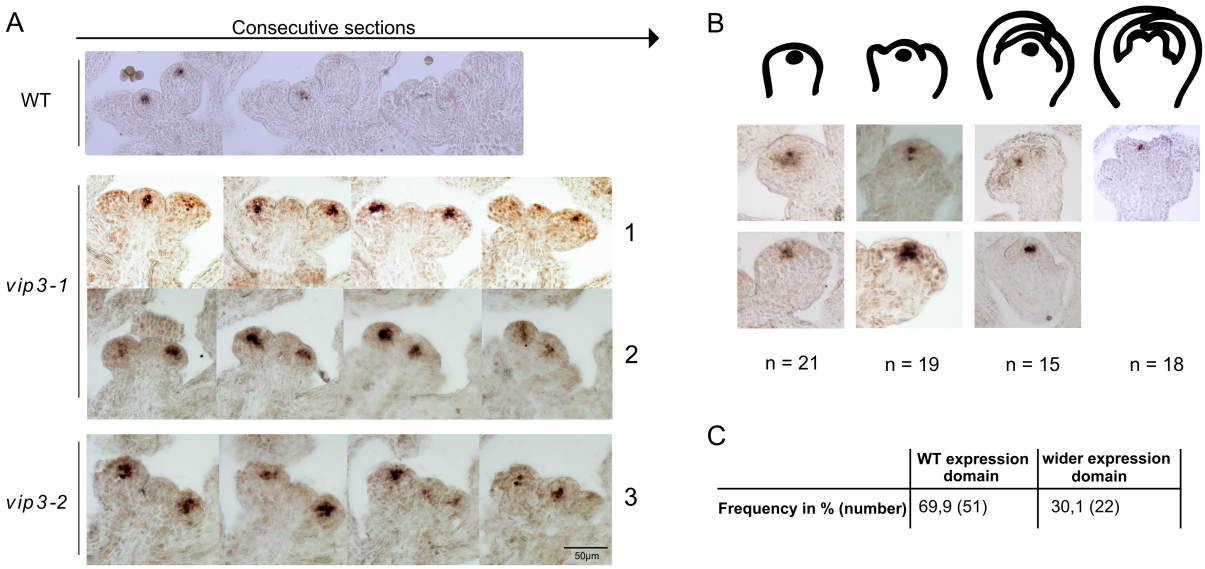

C

	WT expression domain	wider expression domain
Frequency in % (number)	69,9 (51)	30,1 (22)

Fig. S6. Expression patterns of *WUS* in *vip3* flowers.

(A, B) *In situ* hybridization of *WUS* transcripts in wild-type (A, upper panel) and *vip3-1* (A, lower panel and B). (A) Consecutive sections on WT and 3 independent *vip3* (1-2: *vip3-1*; 3: *vip3-2*) apices showing an expansion of *WUS* expression domain in *vip3-1* floral meristems, when compared to wild type. (B) Representative patterns of *WUS* expression domain in *vip3-1* flower buds at four different developmental stages (as represented by schematic drawings). Plants were grown in short day then continuous light 16°C conditions (as in Fig. 1). Scale bar: 50 µm. (C) Number of flower meristems displaying a wild-type *WUS* expression domain and an enlarged *WUS* expression domain in *vip3-1*.

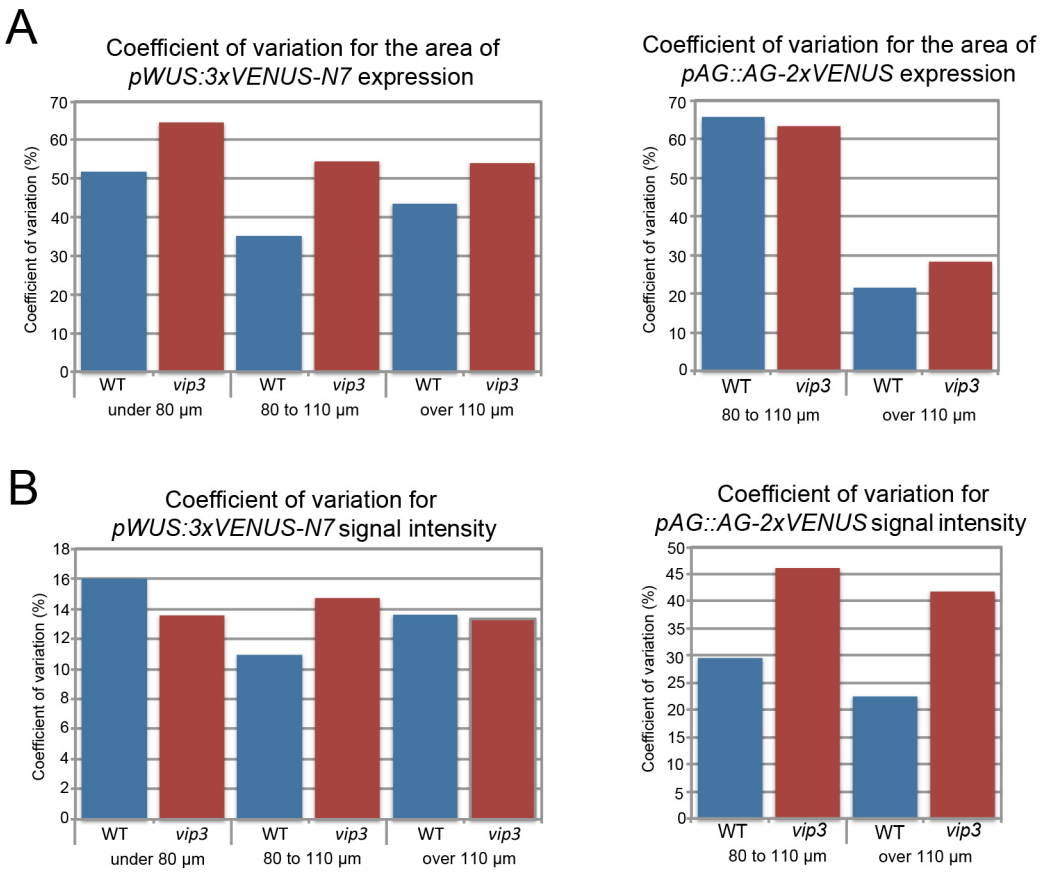

Fig. S7. Coefficient of variation for *WUS* and *AG* expression area and average intensity in *vip3* flowers

(A) Histograms displaying the coefficients of variation (%) for the area of *pWUS::3xVENUS-N7* (left) and *pAG::AG-2xVENUS* (right) expression in wild-type and *vip3-1* flowers. (B) Histograms displaying the coefficients of variation for the average fluorescence signal intensity of *pWUS::3xVENUS-N7* (left) and *pAG::AG-2xVENUS* (right) expression in wild-type and *vip3-1* flowers.

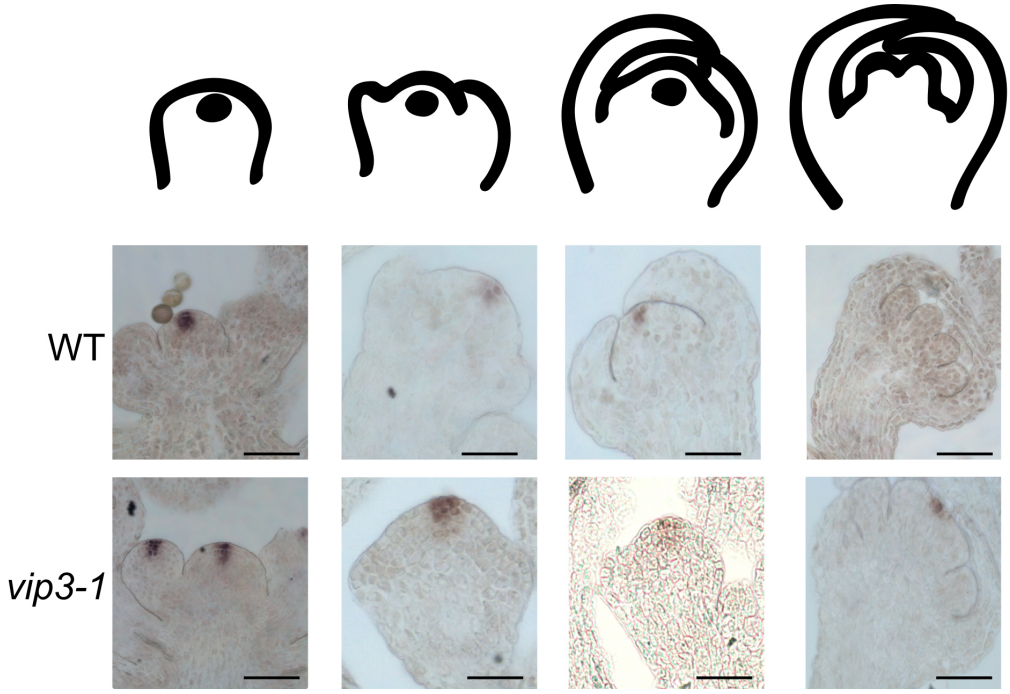

Figure S8. Expression patterns of *CLV3* in *vip3-1* flowers

In situ hybridization of *CLV3* transcripts in wild-type (A) and *vip3-1* (B). Plants were grown in short day then continuous light 16°C conditions (as in Figure 1). Scale bar = 50 µm.

Table S1. List of primers

Name	Sequence
Genotyping primers	
LBb1.3	ATTTTGCCGATTTCGGAAC
vip3-1 F	GACTGCAAGTACCACTTTCGC
vip3-1 R	TAATGGGAAACGACTTGCTTG
vip3-2 F	CTGACTGGATCTCTTGACGAGACG
vip3-2 R	GATACTCAGCAATTCCATATAGTACCCAAGC
Primers for *in situ* probes	
*WUS_in_situ*_F	CAACAAGTCCGGCTCTGGTG
*WUS_in_situ*_RT7	TGTAATACGACTCACTATAGGGCGGGAAGAGAGGAAGCGTACGTCG
*AG_in_situ*_F	ACGGCGTACCAATCGGAGCT
*AG_in _situ*_RT7	TGTAATACGACTCACTATAGGGCGTTGCAATGCCGCGACTTGG
CLV3_in_situ_F	ATGTCCGGTCCAGTTCAACAAC
CLV3_in_situ_RT7	TGTAATACGACTCACTATAGGGCGGTCAGGTCCCGAAGGAACA
Primers for *pAG::AG-2xVenus* construction	
pPD381	GTCCCCGGGAGTGATCCCTTCTCCAACACA
pPD413	AGTCCCGGGTAACTGGAGAGCGGTTTGGT
pPD441	AGTGGATCCGCAGCTGCCGCAGCTGCGATGGTGAGCAAGGGCGAG
pPD442	GTCTCTAGACTAGATAGATCTCTTGTACAGCTC